BUNDLE SHEATH SUBERIN LAYER AS A BARRIER TO RUMEN MICROBIAL DEGRADATION IN INDIANGRASS AND BIG BLUESTEM LEAF BLADES

by

ARTHUR A. HASTERT

B. S., Kansas State University, 1978

A MASTER'S THESIS

submitted in partial fulfillment of the

requirements for the degree

MASTER OF SCIENCE

Department of Agronomy

KANSAS STATE UNIVERSITY
Manhattan, Kansas

1982

Approved by:

Clenton Owensby
Major Professor

TABLE OF CONTENTS

ACKNOWLEDGEMENTS

I sincerely wish to thank the following persons. Their combined contributions to my graduate thinkings are incommensurable with the worth of anything written on paper. Gene Towne and Walt Fick for their teachings, Len Harbers for his enthusiasm, Spencer Tomb for his *simpatico*, Clenton Owensby for his incredibly awesome foresight, guidance, and patience, Mom for her everlasting love, and the Holy Trinity for having dropped all the missing puzzle pieces into my lap.

INTRODUCTION

Studies on the structural barriers to forage leaf digestion which include silica (Harbers et al. 1981; Denium 1974) and lignin (Harbers et al. 1981; Barton and Akin 1977; Akin and Burdick 1973; Van Soest 1968) have indicated that anatomical location of the barrier may be equally as important to consider as amount of barrier when evaluating forage quality. Other barriers to rumen microbial degradation include the phytopolymer, cutin, which makes up the plant cuticle and lines substomatal cavities (Brazle et al. 1979; Hanna et al. 1973; Monson and Burton 1972).

Members of the Gramineae that utilize the C_4 pathway of photosynthesis are characterized by having a distinct internal leaf blade anatomy called Kranz-type (Downton and Tregunna 1968) which may be partly responsible for the relatively low nutritive values associated with these plants. Predominant anatomical characteristics of leaf blades of C_4 grasses that affect rumen microbial degradation patterns of grass leaf tissue are the well-developed parenchyma bundle sheath cells that possess high concentrations of starch-containing chloroplasts. Akin and Burdick (1977) reported that starch remained undegraded in parenchyma bundle sheath cells of warm-season grasses until rumen bacteria were able to disrupt the laminated cell wall of the sheath cells. These authors, as well as others (Harbers and Thouvenelle 1980; Harbers et al. 1981), have reported that mesophyll and phloem tissues usually were degraded earlier than parenchyma bundle sheath cells for both C_3 and C_4 grasses subjected to rumen microbial degradation.

Using transmission electron microscopy (TEM), ultrastructural examinations of parenchyma bundle sheath cells in many C_4 grass species have revealed the existence of a suberized lamella in the cell walls completely

or partially encasing each cell (O'Brien and Carr 1970; Evert et al. 1978; Espelie and Kolattukudy 1979). Suberin has been reported to consist of a phenolic matrix somewhat similar in structure to that of lignin, but differing from lignin in that covalently-bonded aliphatic components prevail (Kolattukudy 1981). Several types of plant tissues have been described as containing suberin, and in most cases observations on the deposition patterns have indicated that the main function of suberin is to act as a biological barrier. Known to exist among these deposits are the Casparian strips found within the cell walls of root endodermis of most vascular plants.

The objectives of this study were to i) estimate the percentages of certain tissues in leaf blades of two warm-season grasses in late spring and late summer and ii) investigate the effect of a suberized layer in parenchyma bundle sheath cells on the *in vivo* degradation patterns by rumen microorganisms on certain leaf blade tissues.

MATERIALS AND METHODS

Plants of indiangrass [*Sorghastrum nutans* (L.) Nash] and big bluestem (*Andropogon gerardi* Vitman) were clipped near ground level on an ungrazed, annually burned (about May 1) loamy upland range site in the Tallgrass Prairie region of the Kansas Flint Hills near Manhattan, Kansas. Clipping dates were May 5 (20 days postemergence) and Sept. 29 (140 days postemergence). Plants were kept cold in an ice bath and transported to the laboratory for leaf cutting. Sections (3 cm in length) were cut and removed from near the midpoint in the leaf blade for those green leaves selected at a standard position along the stem (i.e., second leaf emerged from stem for late-spring plants and leaves midway along the stem for late-summer plants). A device consisting of several single-edged

razor blades positioned approximately 0.5 mm apart was then used to cut the leaf sections longitudinally in such a manner that would least damage vascular bundles. Fifteen to twenty leaf-blade strips, each containing about four to six vascular bundles, were then transferred to each of 42 and 36 polyester monofilament screen cloth bags for late-spring and late-summer digestion trials, respectively. Bag pore size equaled 43 μm (J. Heidkir, pers. comm.). In order to minimize dessication, leaf-blade strips were kept in a beaker, cooled by ice, during the duration of the cutting process.

Polyester bags were tied in groups of two to three to a circular nylon string and then suspended into a mature rumen-cannulated steer grazing late-spring, annually-burned tallgrass prairie. Leaf sections were subjected to rumen incubation for 0, 1, 2, 4, 8, 16, 32, and 64 hr for the late-spring degradation trial, with 96 and 128 hr added for the late-summer degradation trial.

Control intact leaf strips (0 hr of incubation) and digested leaf strips removed from the rumen were cold-fixed in 4% glutaraldehyde in 0.1 m phosphate buffer (pH 7.0) for 3 to 5 hr. After rinsing in cold buffer leaf blade strips were then cut with a razor blade near the middle of the length of the strip to give small (2mm X 0.5mm) sections that would undergo the remaining preparations and observations. Leaf sections were then post-fixed in cold, 1% buffered osmium tetroxide for 2 hr, rinsed in buffer, and then dehydrated in a graded series of ethanol-water washes (50, 70, 95, 100% vol/vol). Following a rinse in 100% propylene oxide, samples were then infiltrated with Mascorro low-viscosity resin (Mascorro et al. 1976) for at least 14 hr before flat embedding in fresh resin. Leaf sections were heated at 70° C for 48 hr to polymerize the resin.

Ultra-thin sections were cut at 60 to 150 nm for transmission electron microscopy and thick sections were cut at about 0.75 μm for light microscopy using a Reichert OMU-2 ultramicrotome. Thin sections were post-stained with 5% uranyl acetate in 50% ethanol for 10 to 15 min, followed by lead citrate for 2 to 5 min, and then observed in the Phillips TEM 201. Thick sections were stained with a 1% aqueous solution of toluidine blue in a 1% aqueous solution of borax (1:1; vol/vol) and then observed with light microscopy.

Areas of various tissue components for undigested leaf blades of both late-spring and late-summer plants were estimated as a percent of the intra-epidermal leaf blade area by using a planimeter to trace outlines of tissues shown in light micrographs of leaf blade cross sections. The inner abaxial and adaxial epidermal walls and boundaries drawn perpendicular between the two epidermal layers were traced to determine an average base planimeter reading (IE) from which all other averaged readings for leaf blade components of that particular section could be subtracted. Average planimeter values were obtained for a circular trace of the inner walls of the parenchyma bundle sheath and constituted the phloem and xylem component (PX). These values were then subtracted from average area readings of a circular trace of the outer walls of the parenchyma bundle sheath (BSPX) so that a value for percent area of parenchyma bundle sheath could be obtained (BSPX - PX/IE x 100 = % BS). Average area values obtained from the planimeter tracings of the outer walls of the parenchyma bundle sheaths (BSPX) were subtracted from the intra-epidermal area values (IE) to obtain percent area values for the mesophyll-sclerenchyma (MS) component (IE - BSPX/IE x 100 = % MS). Percent areas of the phloem-xylem and mesophyll-sclerenchyma components were determined from those micrographs of leaf-blade cross sections having vascular bundles with uninterrupted

bundle sheaths like those described for C_4 grasses by Metcalfe (1960).

Leaf-blade sections from one to as many as four different leaf strips for each rumen-incubation period for each grass species in both late-spring and late-summer digestion trials were observed with light microscopy and amounts of tissues remaining for each leaf-strip sample were visually estimated by assigning values of 4, 3, 2, 1, and 0 for 0, 25, 50, 75, and 100% degradation, respectively. Observations were made on more internally located tissues away from cut ends in order to standardize comparisons of rates of tissue disappearance. Scores were averaged for each incubation time for each grass in both digestion trials.

RESULTS AND DISCUSSION

Composition of Undigested Leaf Tissues

Light micrographs of undigested leaf cross sections for late-spring (20 days postemergence) and late-summer (140 days postemergence) indiangrass and big bluestem plants show representative tissue arrangements used to measure tissue components (Fig. 1, 12). Percent areas of parenchyma bundle sheaths for both grasses in late-spring and late-summer growth stages did not differ greatly between species (range 16.7 to 21.0%). Amounts for late-spring leaf blades were slightly higher (2.4 and 4.3 percentage units higher for indiangrass and big bluestem, respectively) than amounts of parenchyma bundle sheath areas for late-summer cross sections (Table 1). Percent areas of parenchyma bundle sheaths reported here are intermediate to percent areas of parenchyma bundle sheaths for other C_4 grasses reported by Akin and Burdick (1975). Percent areas of bundle sheaths for C_4 grass leaf blades at 4 weeks regrowth reported by these authors ranged from 28.5% for 'Costal' bermudagrass (*Cynodon dactylon* (L.) Pers.) to 9.5% for pangolagrass (*Digitaria decumbens* Stent.).

Percent areas of the mesophyll-sclerenchyma components did not differ greatly between species for any one growth stage (range of 68.0 to 72.4%). Percent areas of the phloem-xylem component ranged from 8.7 to 12.3% and did not differ between any one species or for any one growth stage (Table 2). Percent areas for the mesophyll-sclerenchyma component of indiangrass and big bluestem appear to be greater than for those tissue values combined in other warm-season grasses studied by Akin and Burdick (1975). Had epidermis and bulliform cells been included in the cross section area for determining percentages of tissue components, values would have been lower and perhaps more like those of other C_4 grasses.

Late-spring Digestion Trial

For most incubation times light microscopy observations revealed the aggregation of rumen bacteria immediately inside the open ends of leaf blade sections where cuts had been made earlier. A thin, electron-translucent suberin layer encased all outer tangential and radial walls of parenchyma bundle sheath cells and widened in cell wall regions where pit fields between mesophyll and bundle sheath cells were located (Fig. 2).

Light microscopy examinations of cross sections of leaf strips from late-spring big bluestem and indiangrass plants after 1, 2, 4, and 8 hr of rumen incubation revealed little degradation of tissues (Table 3). Mesophyll and inner epidermal cell walls for both grass species, and the phloem cells of big bluestem showed signs of initial degradation to be between 8 and 16 hr. The observation that degradation of the inner epidermal wall occurs prior to degradation of the outer epidermal wall has been reported for other grasses (Hanna et al. 1973) and demonstrates the potential influence of variability in cell wall thickness or composition within a single tissue type in determining rumen microbial digestion patterns.

Closer examinations with transmission electron microscopy of leaf tissues subjected to 1, 2, and 4 hr of rumen incubation revealed some degradation occurring to cell walls of the mesophyll (Fig. 3, 5). Walls of parenchyma bundle sheath cells for these same digestion times, however, showed no sign of degradation (Fig. 2-6). Peripheral edges of chloroplasts for both mesophyll and parenchyma bundle sheath cells showed signs of deterioration that were not seen in undigested leaf samples (Fig. 3). Numerous starch grains were viewed in bundle sheath cells, but indications of starch hydrolysis were absent for the 1, 2, and 4 hr incubation times. Starch grains within the bundle sheaths of other C_4 grasses subjected to rumen microbial degradation have been reported not to be hydrolyzed until the thick laminated cell walls of the bundle sheaths could be disrupted (Akin and Burdick, 1977). Observations in this study indicated likewise.

After 16 hr of rumen incubation, mesophyll tissue for both grass species was at least 50% degraded (Table 3). Parenchyma bundle sheaths, however, did not reach this state until 32 hr for indiangrass and somewhere between 32 and 64 hr for big bluestem. Only xylem and the other presumably-lignified vascular tissues remained for both species at 64 hr of *in vivo* degradation (Fig. 10).

For those incubation times where mesophyll tissue underwent extensive degradation (e.g. 16, 32 hr) transmission electron microscopy of adjacent mesophyll and bundle sheath walls usually revealed the removal of mesophyll cell wall material, but not the adjacent bundle sheath cell wall material (Fig. 7, 9). Many times degradation of the mesophyll cell wall was extensive enough to expose, but not extend through the suberin layer. In cases where the removal of a large proportion of the bundle sheath cell wall was evident the suberin layer was still intact (Fig. 8, 10, 11).

Table 1. Percent areas of parenchyma bundle sheaths determined from leaf blade cross sections for big bluestem and indiangrass in late-spring and late-summer growth stages.

Species: growth stage	No. of cross sections sampled	No. of vascular bundles sampled	Parenchyma bundle sheath
			% S.D.
Big Bluestem			
late-spring	4	10	21.0 ± 2.9
late-summer	7	23	16.7 ± 3.0
Indiangrass			
late-spring	4	14	19.7 ± 2.4
late-summer	8	27	17.3 ± 2.4

Table 2. Percent areas of other tissue components for big bluestem and indiangrass in late-spring and late-summer growth stages.

Species: growth stage	No. of cross sections sampled	No. of vascular bundles sampled	Vascular tissue*	Mesophyll and Sclerenchyma
			% S.D.	% S.D.
Big Bluestem				
late-spring	4	10	11.5 ± 7.5	68.0 ± 5.3
late-summer	4	12	9.7 ± 3.1	72.4 ± 2.6
Indiangrass				
late-spring	4	14	8.7 ± 1.2	71.6 ± 2.3
late-summer	6	20	12.3 ± 3.6	70.0 ± 2.8

*xylem and phloem

Table 3. *In vivo* rumen degradation of leaf blade tissues for big bluestem and indiangrass plants in the late-spring growth stage.

Big Bluestem	Incubation time, hours						
	1	2	4	8	16	32	64
No. of leaf strips sampled	2	2	2	2	2	3	3
Phloem	4	4	4	4	3	0	0
Mesophyll	4	4	4	4	2	1	0
Inner epidermal wall	4	4	4	4	2	1	0
Outer epidermal wall	4	4	4	4	4	4	0
Parenchyma bundle sheath	4	4	4	4	4	3	0
Xylem	4	4	4	4	4	4	4

Indiangrass	Incubation time, hours						
	1	2	4	8	16	32	64
No. of leaf strips sampled	2	2	2	3	2	3	3
Phloem	4	4	4	4	4	0	0
Mesophyll	4	4	4	3	1	0	0
Inner epidermal wall	4	4	4	4	1	0	0
Outer epidermal wall	4	4	4	4	4	2	0
Parenchyma bundle sheath	4	4	4	4	3	2	0
Xylem	4	4	4	4	4	4	4

4 = not degraded, 3 ≅ 25% degraded, 2 ≅ 50% degraded, 1 ≅ 75% degraded, and 0 = 100% degraded.

Figure 1. Light micrograph of a cross section of an undigested leaf blade from an indiangrass plant (20 days postemergence) showing a similar arrangement of tissues as those used to estimate tissue areas. Epidermis was not included in calculations as part of the leaf area because of the numerous large air-filled bulliform cells that would have considerably reduced estimates. PBS, parenchyma bundle sheath; abe, abaxial epidermis. Bar = 50 µm.

Figure 2. Transmission electron micrograph of a pit field between a mesophyll cell (MC) and a bundle sheath cell (BSC) from an indiangrass leaf blade. A suberin layer (arrows) in the outer tangential wall of the bundle sheath cell appears to widen in the area of the pit field and encase each plasmodesma. Bar = 0.5 µm.

Figure 3. Transmission electron micrograph showing the typical radial orientation of 2-3 mesophyll cells (MC) against a single bundle sheath cell (BSC) taken from an indiangrass leaf blade sample (20 days postemergence) after 1 hr of rumen incubation. Numerous starch grains (SG) are present within the bundle sheath cell, but are lacking in mesophyll. Bar = 2 µm.

Figure 4. Bundle sheath cell (BSC) with adjacent vascular cells observed by transmission electron microscopy taken from a cross section of a big bluestem leaf sample (20 days postemergence) after 1 hr of *in vivo* degradation. Numerous bacteria are present in one cell of the phloem tissue. SG, starch grains. Bar = 2 µm.

Figure 5. Transmission electron micrograph of an outer tangential bundle sheath cell wall (BSCW) from an indiangrass leaf sample (20 days postemergence) after 2 hr of rumen incubation. The mesophyll cell wall shows some sign of hydrolysis, but beyond the prominent suberin layer (arrows) the bundle sheath cell wall appears to be unaffected. MC, mesophyll cell. Bar = 0.2 µm.

Figure 6. Adjacent cell walls from a bundle sheath cell and a cell of the xylem tissue from a big bluestem leaf blade (20 days postemergence) as revealed by TEM. Note the gradual disappearance of the suberin layer (in the areas between the upper two arrows and below the lower arrow) as it becomes closer in proximity to the xylem cell. Thickness of the suberin layer is relatively narrower in these walls as compared to outer tangential walls of the parenchyma bundle sheath (see Figure 5 taken at a lower magnification). Bar = 0.2 µm.

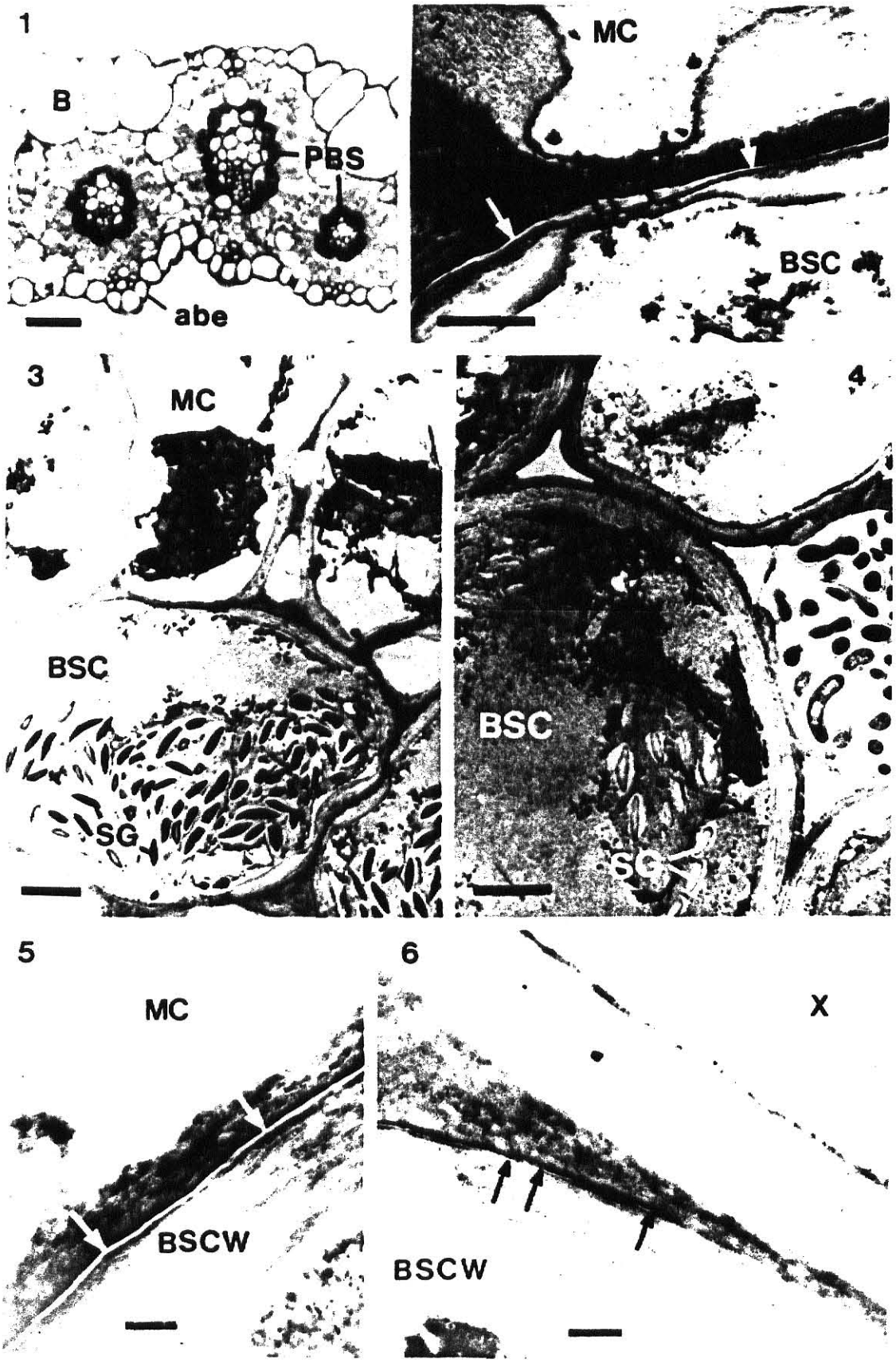
1
B
PBS
abe
MC
BSC
3
MC
BSC
SG
4
BSC
SG
5
MC
BSCW
6
X
BSCW

Figure 7. Bacterial degradation of cell wall material occurring outside the suberin layer (arrow) of an outer tangential bundle sheath cell wall (BSCW) as revealed by transmission electron microscopy. The sample is from a leaf blade strip of big bluestem (20 days postemergence) subjected to 16 hr of incubation. Bar = 0.2 μm.

Figure 8. Transmission electron micrograph showing extensive degradation to a bundle sheath cell (BSC) of an indiangrass leaf blade strip (20 days postemergence) after 16 hr of rumen incubation. One relatively large starch grain (SG) remains while scant amounts of cell wall material are still fixed to the suberin layer as evident by certain regions in the cell wall (arrow). Bar = 0.5 μm.

Figure 9. Transmission electron micrograph showing removal of cell wall material of a mesophyll cell (MC) and removal of middle lamella next to an outer tangential wall of a bundle sheath cell (BSG). Degradation appears to have ended abruptly upon encountering the suberin layer (arrow). The sample is of a big bluestem leaf strip (20 days postemergence) after 32 hr of rumen incubation. Bar = 0.2 μm.

Figure 10. Light micrograph of a vascular bundle from an indiangrass leaf sample (20 days postemergence) after 32 hr of *in vivo* degradation. Radial walls (arrows) of the parenchyma bundle sheath cells remain. Note the large spaces created by the metaxylem vessels (mx), protoxylem lacunae (pxl), and degraded phloem (p). Bar = 20 μm.

Figure 11. High magnification of the remains of cell wall material and associated suberin from a parenchyma bundle sheath cell wall in a big bluestem leaf sample (20 days postemergence) after 64 hr of rumen degradation. Bar = 50 nm.

Figure 12. Light micrograph of an undigested leaf blade cross section from big bluestem (140 days postemergence) showing Kranz type anatomy of one large lateral vascular bundle and two small lateral vascular bundles. bs, bundle sheath; p, phloem; pxl, protoxylem lacunae; mx, metaxylem, s, sclerenchyma. Bar = 50 μm.

Figure 13. Numerous starch grains (sg) within a bundle sheath cell (BSC) revealed by transmission electron microscopy from an undigested leaf strip of indiangrass (140 days postemergence). Bar = 2 μm.

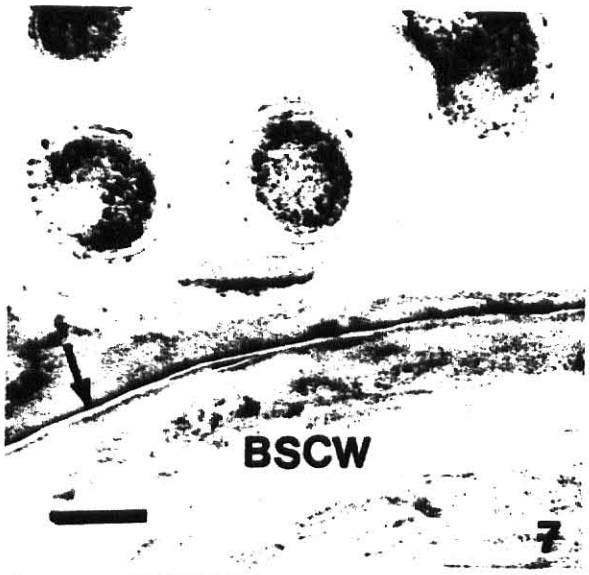

7

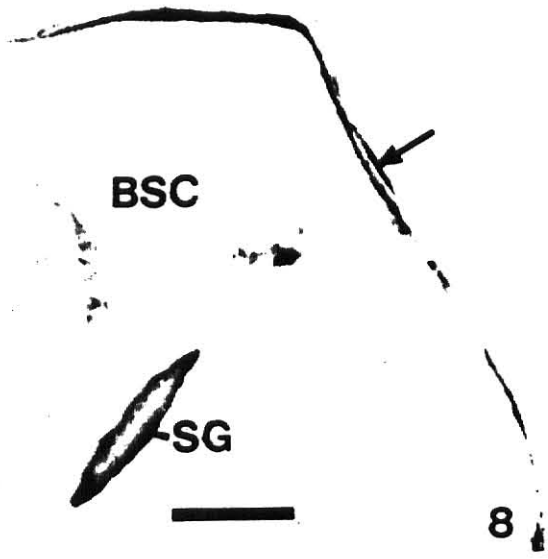

8

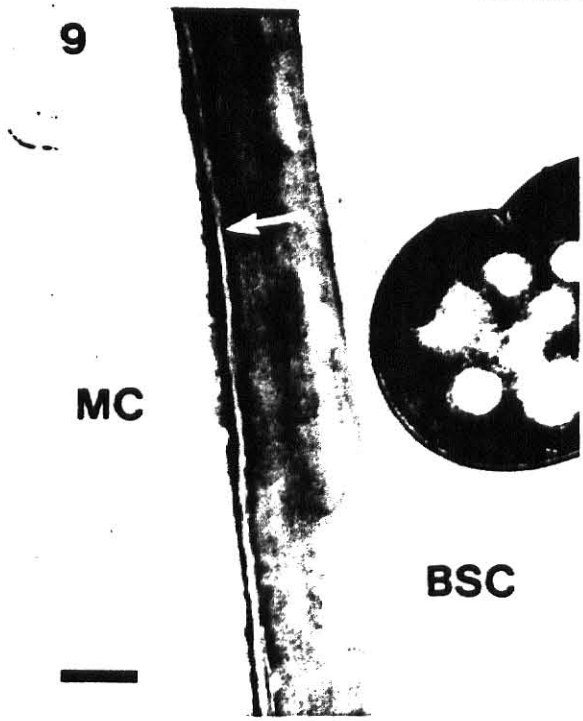

9

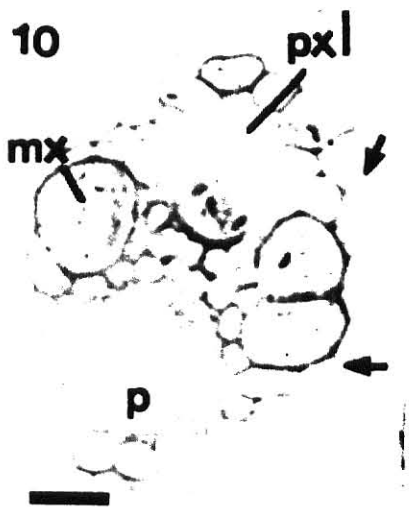

10

11

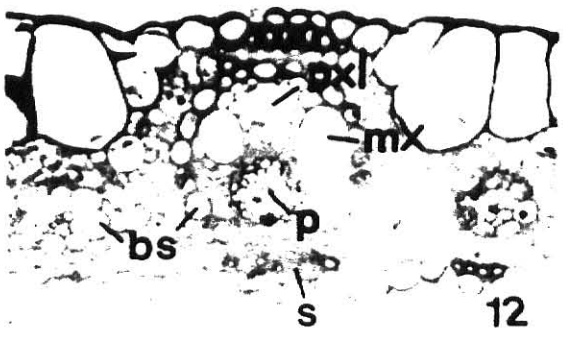

12

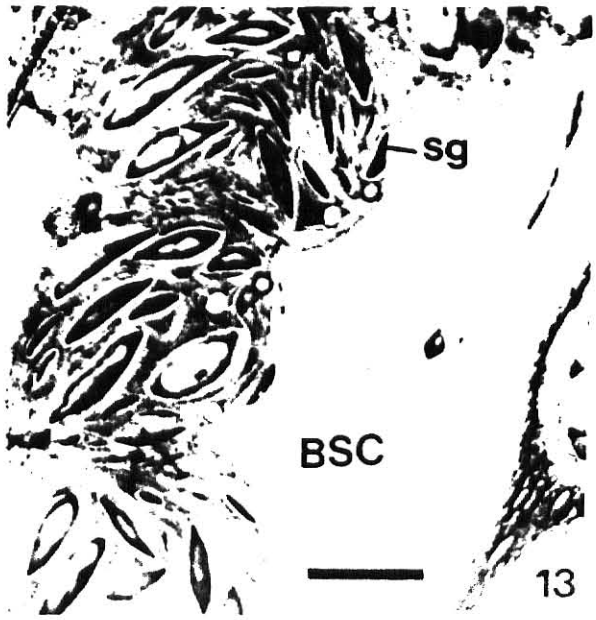

13

Late-summer Digestion Trial

Observations by transmission electron microscopy on leaf blade cross sections of big bluestem and indiangrass plants clipped in late-summer (140 days postemergence) revealed abundant starch grains within parenchyma bundle sheath cells (Fig. 13). Rates of tissue removal for both grasses in the late-summer digestion trial followed the same general sequence of that in the late-spring trial (mesophyll and phloem > parenchyma bundle sheath and epidermis > vascular elements), but the extent of removal tended to be less for similar incubation times. Mesophyll tissue that was 50% degraded at 16 hr or less for both grasses in the late-spring trial was not 50% degraded in the late-summer trial until 32 hr and 96 hr for indiangrass and big bluestem, respectively (Table 4). Similarly, parenchyma bundle sheaths remained 50% or more intact for both grasses in late-summer growth stages for all incubation times except one (indiangrass bundle sheath tissue at 64 hr was 75% degraded) whereas the late-spring values of degradation for bundle sheaths of either grass was 100% by 64 hr.

Transmission electron microscopy of cell walls common to bundle sheath cells and mesophyll cells in both indiangrass and big bluestem leaf sections revealed some similarities in microbial degradation patterns to those observed in the late-spring digestion trials. When the removal of cell wall material was observed for either bundle sheath cell wall or mesophyll cell wall, exposure of the suberin layer was frequent, but degradation of the material opposite the side of the suberin layer where hydrolysis occurred was seldom seen (Fig. 15-17). These observations may indicate hindered penetration of microbial enzymes, but differences in cell wall structure and composition cannot be excluded as contributing factors for differential rates of cell wall hydrolysis across the suberin layer. Espelie and Kolattukudy (1979) used combined gas-liquid chromatography

and mass spectrometry to identify major aliphatic components of the polymeric lipid in the bundle sheath cells of *Zea mays* leaves and found several to be in common with those of the cutin polymer from the cuticle of the same plant. Cuticle has been shown to be indigestible to rumen microbes (Brazle et al. 1979; Hanna et al. 1973), but because it has usually been observed to slough away from underlying epidermis tissue during prolonged rumen incubation, epidermal cell wall surfaces eventually become exposed to bacterial attack. The suberin layer in parenchyma bundle sheath cells, however, is a more permanent structure as evidenced by being embedded between cell walls and may prove to be a more significant barrier to the degradation of internal leaf tissues mainly because of the additional bilateral effect on microbial degradation.

In certain cases for the late-summer digestion trials some estimates of the extent of tissue removal were greater for shorter incubation periods than for longer incubation periods (Table 4). For example, at 64 hr of incubation parenchyma bundle sheath degradation for both grass leaf blades were relatively high (25 and 75% degraded for big bluestem and indiangrass, respectively). After 96 hr of incubation, however, extents of degradation for bundle sheaths were low (0 and 25% degraded for big bluestem and indiangrass, respectively). Phloem tissue for both grasses responded similarly. At 96 hr for big bluestem and at 128 hr for indiangrass amounts of phloem tissue remaining were greater than for the shorter incubation times. These results can be explained if the types of vascular bundles examined in both short and long incubation periods are taken into account. Light microscopy of the leaf blade samples subjected to the longer incubation periods revealed the presence of only the more-developed, large vascular bundles. Small, less-developed vascular bundles that had been observed and included as part of the evaluation of percent degradation in shorter digestion

Table 4. *In vivo* degradation of leaf blade tissues for big bluestem and indiangrass plants in late-summer growth stage.

Big bluestem	Incubation time, hours								
	1	2	4	8	16	32	64	96	128
No. of leaf strips sampled	1	1	1	2	1	3	3	4	3
Phloem	4	4	4	2	2	1	0	1	0
Mesophyll	4	4	4	4	3	3	4	2	0
Inner epidermal wall	4	4	4	4	4	1	2	1	0
Outer epidermal wall	4	4	4	4	4	4	3	2	0
Parenchyma bundle sheath	4	4	4	4	4	3	3	4	3
Xylem	4	4	4	4	4	4	4	4	4
Indiangrass	Incubation time, hours								
	1	2	4	8	16	32	64	96	128
No. of leaf strips samples	2	2	2	2	4	4	4	3	4
Phloem	4	4	4	4	3	2	0	0	3
Mesophyll	4	4	4	4	3	2	2	1	1
Inner epidermal wall	4	4	4	4	3	2	1	0	0
Outer epidermal wall	4	4	4	4	4	4	4	2	0
Parenchyma bundle sheath	4	4	4	4	3	3	1	3	2
Xylem	4	4	4	4	4	4	4	4	4

4 = not degraded, 3 ≅ 25% degraded, 2 ≅ 50% degraded, 1 ≅ 75% degraded, and 0 = 100% degraded.

periods were usually not present for other incubation times because of their tendency to be degraded relatively early (Fig. 18). Hence, estimates of tissue removal for leaf blade samples at longer incubation times represent mainly the large and more-developed vascular bundles causing degradation rates of certain tissues to appear low.

Because a large proportion of the mesophyll tissue remained in samples for both grasses for most of the late-summer incubation periods, rumen bacteria may be somewhat restricted from this tissue by some plant anatomical structure. Brazle et al. (1979) using scanning electron microscopy observed intact spongy mesophyll for big bluestem leaf blades (109 days postemergence) subjected to 72 hr of rumen incubation. In this study, examinations of the remains of small vascular bundles and their surrounding tissues by light microscopy revealed extensive loss of xylem, phloem and parenchyma bundle sheaths, but not of surrounding mesophyll for those leaf blade samples subjected to 32 and 64 hr of rumen digestion (Fig. 18). The reason some vascular bundles were thoroughly digested while the surrounding mesophyll remained intact is most likely due to differential quantities or qualities of cell wall material, anatomical design, or a combination of these factors. Hanna et al. (1973) observed higher degrees of degradation for loosely-arranged mesophyll cells than for more compactly arranged mesophyll cells leaf sections of different pearl millet [*Pennisetum typhoides* (Burm) Stapf and C.E. Hubb] inbreds subjected to the same lengths of *in vivo* digestion with rumen fluid. Akin and Burdick (1981) recently applied different histochemical tests for lignin to tissues of grass leaf blades and were able to relate resistance to *in vivo* rumen digestion with positive staining reactions by chlorine-sulfite and acid phloroglucinol. Portions of the mesophyll and parenchyma bundle sheath of Kentucky-31 tall fescue (*Festuca arundinacea* Schreb.) that resisted 24 to 72 hr of rumen

incubation stained positive for lignin with chlorine-sulfite.

Transmission electron microscopy of the cell walls common to bundle sheath cells and mesophyll cells for the smaller vascular bundles of late-summer samples after 32 and 64 hr of incubation revealed the removal of a large proportion of the bundle sheath secondary cell walls. A suberin layer still attached via primary wall of the parenchyma bundle sheath and adjacent middle lamella to walls of the mesophyll was present for these bundles (Fig. 19). Observations of intact vascular bundles in leaf samples subjected to shorter incubation periods for either digestion trial revealed portions of the inner tangential walls of bundle sheath cells containing a suberin layer, but as the bundle sheath cells walls and adjacent cell walls of the xylem or phloem tissues converged to more tighter associations, the suberin layer became absent (Fig. 6, 14). The absence or presence of a suberin layer in bundle sheath cell walls adjacent to the walls of vascular tissue may depend upon several factors of which type of vascular bundle and particular type of adjacent vascular tissue are major. Evert et al. (1978) observed leaf cross sections of *Zea mays* and reported the presence of a continuous suberin layer in the outer tangential and radial walls of the bundle sheath cells for small and intermediate longitudinal bundles, but inner tangential cell walls, and specifically those inner walls contiguous to companion cells and thin-walled sieve tubes of the phloem, were only partly suberized. Transverse veins, however, showed that inner tangential walls of bundle sheath cells contained well-developed suberin layers opposite the sieve tubes and parenchymatic vascular elements. For inner tangential walls of these cells in these bundles suberin layers were found only in scattered portions of the wall when walls of the xylem vessels were abutting.

Larger, more-developed vascular bundles in leaf samples subjected to longer incubation periods in the late-summer digestion trial contained mostly intact parenchyma bundle sheath cell walls. A suberin layer could be detected on the outer tangential perimeters of these bundle sheath cell walls and zones of hydrolysis appeared to be prevented from spreading inward to the underlying bundle sheath cell wall material (Fig. 20).

If entry of rumen bacteria into parenchyma bundle sheath cells is prevented in some cases by a suberin layer in the cell walls, then those areas in the cell wall where suberin is lacking (i.e. walls abutting vascular tissues) may prove to be less restricting to bacterial degradation and access to internal starch nutrients could be permitted. Observations in this study support that hypothesis at least for the smaller vascular bundles of C_4 grasses in later growth stages. Provided that cut ends of leaf blades are available in the rumen, vascular bundles may function as avenues for relatively quick bacterial distribution. Coupled with the deterrent to digestion that a compact spongy mesophyll provides, initial patterns of bacterial degradation via open vascular channels may prove to be a significant pathway for microbial entry and subsequent digestion of C_4 grasses. Plant microanatomy has a direct and important impact on microbial digestion.

Figure 14. Transmission electron micrograph of a pit field connecting a cell of the xylem with a parenchyma bundle sheath cell (bsc) observed in an indiangrass leaf sample (140 days postemergence) that was subjected to 1 hr rumen degradation. No suberin layer is apparent. Bar = 0.2 μm.

Figure 15. Transmission electron micrograph revealing rumen microbial degradation occurring to a mesophyll cell wall (MCW) in a big bluestem leaf sample (140 days postemergence) after 8 hr of rumen incubation. Note that the suberin layer (white arrow) appears to be contiguous with the curvature of the bundle sheath cell wall (bscw) and that bacterial degradation did not extend into the bundle sheath cell wall at the point where the suberin layer became exposed (black arrow). Bar = 0.5 μm.

Figure 16. Transmission electron micrograph of bundle sheath cell wall (bscw) and suberin layer (arrow) remaining after the removal of mesophyll tissue (m) in a big bluestem leaf sample (140 days postemergence) subjected to 8 hr of rumen incubation. The middle lamella appears to have been degraded. Bar = 0.2 μm.

Figure 17. Transmission electron micrograph showing portions of two adjacent bundle sheath cell walls (bscw) where middle lamellae (ml) and suberin layers (arrows) remain, but the cell wall material of one bundle sheath cell is absent. The sample is of an indiangrass leaf strip (140 days postemergence) subjected to 32 hr of *in vivo* degradation. Bar = 0.5 μm.

Figure 18. Light micrograph of a small lateral vascular bundle and surrounding tissue in a leaf blade cross section from a big bluestem sample (140 days postemergence) after 64 hr of rumen degradation. Mesophyll tissue shows relatively little disruption. Extensive degradation has occurred to the parenchyma bundle sheath (bs) and xylem and phloem tissues, however. Bar = 20 μm.

Figure 19. Transmission electron micrograph showing high magnification of the remains of a bundle sheath cell (bsc) bordering mesophyll tissue in a small lateral bundle similar to the one depicted in Figure 18. Note that the attachment of the suberin layer (arrow) to the hydrolyzed wall (hw) of the mesophyll appears to be contiguous with the shape of the pre-existing bundle sheath cell. The sample is of a leaf blade strip from big bluestem (140 day postemergence) after 96 hr of *in vivo* degradation. Bar = 0.2 μm.

Figure 20. Transmission electron micrograph of an outer tangential bundle sheath cell wall (bscw) and attached suberin layer (arrow) taken from a large lateral vascular bundle in a leaf blade strip of indiangrass (140 days postemergence) after 128 hr of rumen degradation. Bar = 0.2 μm.

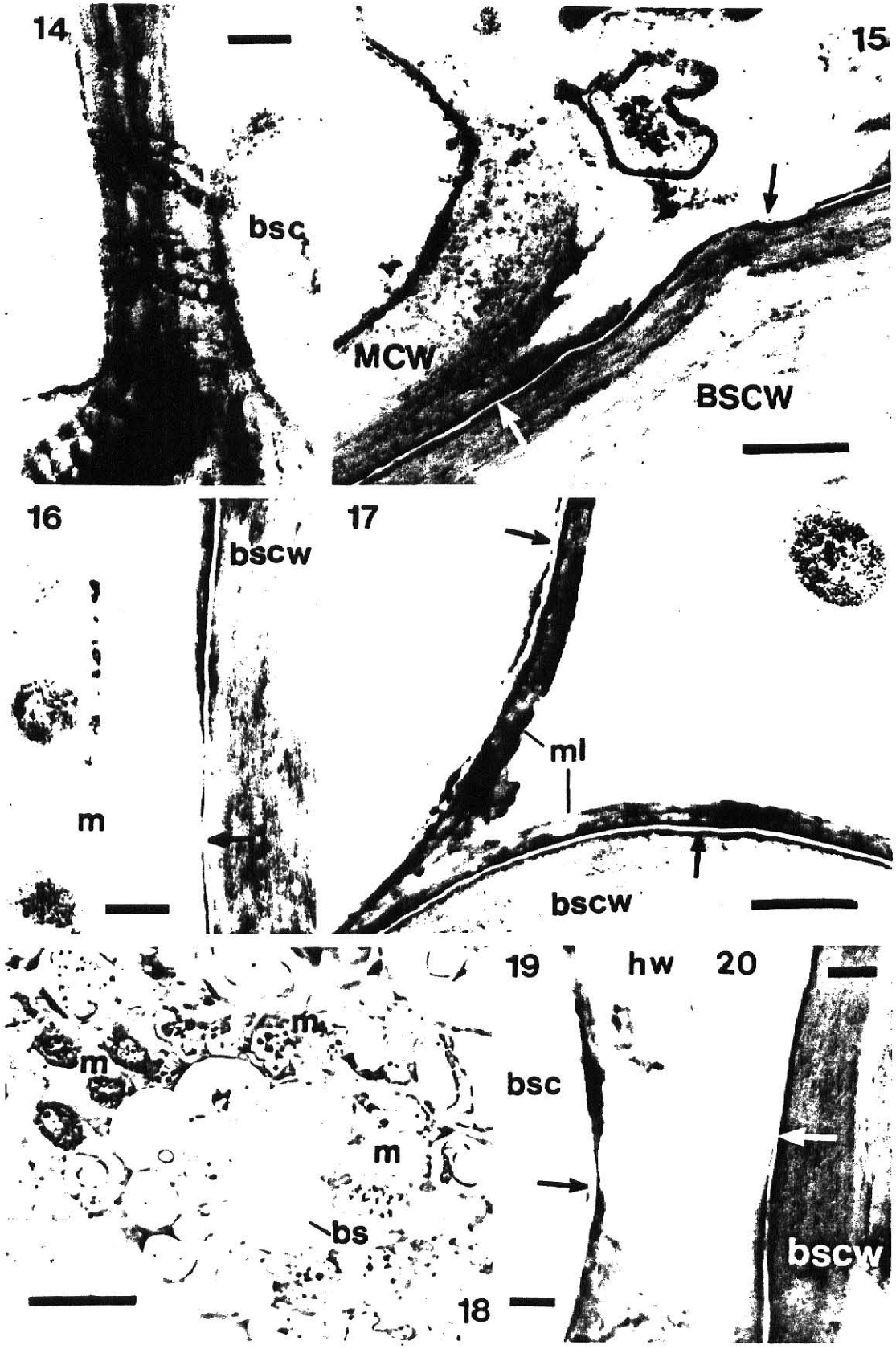
14
bsc
15
MCW
BSCW
16
m
bscw
17
ml
bscw
m
m
m
bs
18
19
hw
bsc
20
bscw

LITERATURE CITED

Akin, D.E. and D. Burdick. 1981. Relationships of different histochemical types of lignified cell walls to forage digestability. Crop Sci. 21:577-581.

Akin, D.E. and D. Burdick. 1977. Rumen microbial degradation of starch-containing bundle sheath cells in warm-season grasses. Crop Sci. 17:529.

Akin, D.E. and D. Burdick. 1975. Percentage of tissue types in tropical and temperate grass leaf blades and degradation of tissues by microorganisms. Crop Sci. 15:661.

Akin, D.E. and D. Burdick. 1973. Microanatomical differences of warm-season grasses revealed by light and electron microscopy. Agon. J. 65:533.

Barton, II, F.E. and D.E. Akin. 1977. Digestibility of delignified forage cell walls. J. Agric. Food Chem. 25:1299.

Brazle, F.K., L.H. Harbers, and C.E. Owensby. 1979. Structural inhibitors of big and little bluestem digestion observed by scanning electron microscopy. J. Anim. Sci. 48:1457.

Denium, B. 1974. Structural inhibitors of quality in forage. Växtodling 28:42.

Downton, W.J.S. and E.B. Tregunna. 1968. Carbon dioxide compensation--its relation to photosynthetic carboxylation reactions, systematics of the Gramineae, and leaf anatomy. Can. J. Bot. 46:207.

Espelie, K.E. and P.E. Kolattukudy. 1979. Composition of the aliphatic components of 'suberin' from the bundle sheaths of *Zea mays* leaves. Plant Sci. Letters 15:225.

Evert, R.F., W. Eschrich, and W. Heyser. 1978. Leaf structure in relation to solute transport and phloem loading in *Zea mays* L. Planta 138:279.

Hanna, W.W., W.G. Monson, and G.W. Burton. 1973. Histological examination of fresh forage leaves after *in vitro* digestion. Crop Sci. 13:98.

Harbers, L.H., F.K. Brazle, D.J. Raiten, and C.E. Owensby. 1981. Microbial digestion of smooth brome and tall fescue observed by scanning electron microscopy. J. Anim. Sci. 51:439.

Harbers, L.H. and M.L. Thouvenelle. 1980. Digestion of corn and sorghum silage observed by scanning electron microscopy. J. Anim. Sci. 50:514.

Heidkir, J. 1981. Personal Communication. Graduate Student, Dept. of Grain Science and Industry. Kansas State University, Manhattan, Kansas.

Kolattukudy, P.E. 1981. Structure, biosynthesis, and biodegradation of cutin and suberin. Ann. Rev. Plant Physiol. 32:539.

Mascorro, J.A., M.W. Ladd, and R.D. Yates. 1976. Rapid infiltration of biological tissues utilizing n-hexenyl succinic anhydride (HXSA)/ vinyl cyclohexene dioxide (VCD), an ultra-low viscosity embedding medium. 34th Ann. Proc. E.M.S.A., 346-347.

Metcalfe, C.R. 1960. Anatomy of the monocotyledons, I. Graminae. Oxford Univ. Press, London. 731 pp.

Monson, W.G. and G.W. Burton. 1972. Effects of length of cut and leaf surface treatments on digestibility of fresh forage. Agron. J. 64:405.

O'Brien, T.P. and D.J. Carr. 1970. A suberized layer in the cell walls of the bundle sheath of grasses. Aust. J. Biol. Sci. 23:275.

Van Soest, P.J. 1968. Structural and chemical characteristics which limit the nutritive value of forages. In "Forage, Economics-Quality." Special Publication 13, Am. Soc. Agron., Madison, Wisc., 63-76.

APPENDIX

A REVIEW OF THE LITERATURE I. THE COMPOSITION, ULTRASTRUCTURE, NATURAL OCCURRENCE, AND PHYSIOLOGICAL SIGNIFICANCE OF SUBERIN

Of the many compounds that plants require for growth and survival, waxes, cutin, and suberin function predominantly to coat and protect the plant from its external environment. Components of these compounds along with fats, oils, phospholipids and glycolipids are collectively grouped under the class of compounds called lipids which are rich in carbon and hydrogen, soluable in organic solvents, and insoluable in water. The structural polymer, cutin, is a component of the cuticle which functions as the protective coating of most aerial parts of plants. The polymeric material called suberin, however, functions as a biological barrier in a variety of plant organs. The following is a review on the composition, ultrastructure, natural occurrence, and physiological significance of suberin.

Dermal Tissue

When cross sections of roots from vascular plants are examined microscopically, a specialized layer of cells called the endodermis can usually be seen separating the central conducting vessels from the root cortex. Upon maturation of the primary vascular tissues, radial and transverse cell walls of the endodermis start to develop a narrow band termed the Casparian strip. These strips are chemically unrelated to the other components of the cell wall as shown by stains specific for lignin and suberin.

Using transmission electron microscopy (TEM), Bonnett (1968) described the Casparian strip in the endodermis of *Convolvulus arvensis* as being situated medianly in the radial walls and occupying a space about one-third the length of these walls. Prior to fixation in glutaraldehyde, root sections

were treated with a 2% aqueous solution of glycerin for 15 minutes. Upon microscopic examination, plasmolysis was seen to occur in all endodermal cell regions except for those of the suberized wall. Here, the plasmalemma failed to separate from the cell wall suggesting the existence of a remarkable affinity between plasmalemma and Casparian strip. Because Casparian strips of one endodermal cell are coincident to adjacent endodermal cells, and because the endodermis is a continuous sheath surrounding the stele, the tenacious affinity between plasmalemma and Casparian strip helps create a physiological barrier to apoplastic movement of water and solutes in a direction from cortex to stele.

Robards et al. (1973) observed the endodermal cells in cross sections of barley roots and reported in addition to Casparian strips in the radial walls an asynchronous deposition of thin opaque suberin lamella that lined the interior of all endodermal wall surfaces. That stage in endodermal development has been considered a secondary state, and for some species it normally follows the development of Casparian strips or primary state (Esau, 1965). The uneven deposition of thick cellulosic wall layers along the inner tangential and radial walls (tertiary state) of the endodermis was reported in barley roots (Robards et al. 1973) and is a common development (following state II) to the monocotyledons (Esau, 1965). By using radioactive strontium, ^{85}Sr, as a tracer for calcium, Robards et al. (1973) were further able to demonstrate a close correlation with long distance transport of calcium from cortex to stele and the incidence of suberin lamella in the endodermal cells. Because plasmodesmatal frequences were comparable in both radial and tangential walls, these authors concluded that apoplastic movement of calcium into the stele was effectively prevented by suberin lamella leaving movement via the symplasm as the only alternative.

Wilson and Robards (1978) demonstrated differential patterns of development for suberized endodermis in response to environmental resistance. These researchers observed suberization of endodermal cells occurring much earlier in the primary development of the root tissue for roots of barley growing under an artificially-induced mechanical constraint when compared to unimpeded roots. At 20 mm from the root apex only about 10% of the endodermal cells for unimpeded roots developed into secondary and tertiary states, whereas at 15 mm from the root tip only 13% of the endodermal cells for impeded roots remained in the primary state of development. In contrast to the normal development of secondary and tertiary states of endodermal cells at basal regions of unimpeded roots, only about 85% of the endodermal cells at the basal regions of impeded roots remained in the primary development state. The authors claimed that since basal regions of impeded roots were not subjected to the same pressure to which apical regions were subjected, then the observations made were evidence for an endodermal capacity for responding to different lateral pressures exerted along the root axis as well as to apical stimulus.

In some circumstances the suberization process, depending upon the plant tissue, appears to have a differential effect on the movement of ions. Development of suberin deposits in the endodermis of maize roots had little effect on the transport of phosphate (Ferguson and Clarkson, 1975). In the basal root sections of ten-day-old maize seedlings, however, the development of suberin in the hypodermis, a specialized layer of cells directly underlying the epidermis and distinct from cortical cells, allowed very little radial movement of phosphate (Ferguson and Clarkson 1976). In contrast, observations of basal root sections of

barley hypodermal cells showed no development of suberized lamella and the restriction of phosphate movement did not occur.

Tippet and O'Brien (1976) described the ultrastructure of the hypodermis in roots of two eucalypt species that differ in their susceptibility to the pathogen *Phytophthora cinnamomi* Rands. Broad bands of suberin having a lamellate structure were observed completely lining all walls of the hypodermal cells in both *Eucalyptus obliqua* and *E. st johnii*. Higher concentrations of vascular polyphenols, however, were observed in the hypodermis of *E. st johnii* roots than in the hypodermis of *E. obliqua*. Consequently, they suggested that the greater resistance of *E. st johnii* to *P. cinnamomi* may be due to a lower attraction of the pathogen to the more highly suberized and lignified fine roots in *E. st johnii*. They also compared observations on suberized hypodermis with the observations by Schnepf (1974) on suberized neck cells of secretory glands and implied a similar function of restricting the outward movement of water and backflow of excreted material for the suberized lamella in the hypodermis of roots.

Suberized lamella may partly contribute to a plants' efficiency in water loss regulation. Olesen (1978) microscopically examined exodermis cells in roots of *Hoya carnosa* L. and observed short cells that were unsuberized sometimes alternating with long cells that were suberized. The long cells were observed to develop a structure of 5-25 electron-translucent suberin lamellae embedded in a slightly denser matrix material completely encasing the entire cell. These observations of suberin lamella corresponded very well with those of Tippet and O'Brien (1976). Typical tertiary wall deposition occurred following suberin deposition. The unsuberized short cells of the exodermis were coincident to root hair

regions and were characterized by a thickened outer tangential wall containing many tortuous channels. Through microanatomical examination of these short cells, Olesen (1978) was able to postulate a regulatory mechanism in which the prominent channels of the outer wall of the short cell would close off or open up transport pathways between epidermis and exodermis depending upon relative states of hydration or dehydration. That mechanism, aided by the long cell suberization, would increase a plants'ability to effectively balance the changes in water flux.

Apparently, suberization of some tissues may prevent flow of water, but in other tissues it may have no effect on water movement at all. Peterson et al. (1978) provided histochemical and ultrastructural evidence for the presence of suberin in onion root hypodermis and epidermis. These regions autofluoresced yellow indicating the presence of suberin or lignin. Phloroglucinol tests were negative for lignin for both of these tissues. Both long and short cells were observed in the hypodermis and at 10 cm from the root tip both cell types were suberized. Hypodermal cells when examined with TEM possessed a multilayered structure of alternating osmiophilic and osmiophobic lamella suggested by the authors to represent the presence of suberin and wax, respectively. Authors reported a similarity in structure between the suberin lamella completely encircling the hypodermal cells and the endodermal cells in secondary development reported elsewhere (Clarkson and Robards 1975, Robards et al. 1973). When tissues were fixed in glutaraldehyde-ferric chloride, the layers of suberin lamella in the hypodermis became less distinct and the subsequent binding of ferric ions made the radial walls of the hypodermis very electron-opaque, thus indicating the presence of polyphenols. Epidermal cell walls lacked suberin lamella, but were believed to contain a non-lamellar form of

suberin interspersed with other wall components due to several factors. Among these factors were histochemical identification of suberin and not cutin and the resistance to concentrated sulphuric acid digestion. Hypodermal cell walls, but not epidermal cell walls, proved to be a barrier to the movement of Uvitex CFX, a high molecular weight (813) fluorescent dye, and authors concluded that water and ions would normally be taken up by onion epidermal cells and made available to at least the symplast of hypodermal cells.

Schonherr and Ziegler (1980) demonstrated impermeability of suberized periderm cells to water flow in *Betula* periderm. Heavily-suberized cells that lacked intercellular spaces were described. Authors were able to determine that the main water flow was via middle lamella and primary cell walls as indicated by polarity from toluidine blue staining and to the occurrence of silver ions, when added as a tracer, in the middle lamella, primary cell walls, and plasmodesmata regions, but not in the suberized walls.

Dean et al. (1977) examined the ultrastructure of suberized regions in the potato tuber skin, wound-healing periderm, and the tissue lining the internal "hollow heart" areas and observed remarkable similarities in the multilayering structures of the cell walls for all of these tissues. Kolattukudy and Dean (1974) identified octadec-9-ene-1,18-dioic acid and 18-hydroxy-octadec-9-encoc acid as some of the major members of the aliphatic component of the wound periderm in potato tuber slices and used the presence of these bifunctional C_{18} molecules in wound periderm to correlate the development of resistance to water loss in the potato slices. As a result, a direct proportion of the quantity of these molecules to the resistance of water loss was produced. Authors suggested a dual function

of suberin to be the resistance to pathogen entry provided by the phenolic components while the prevention of water loss would be provided by the aliphatic components.

Secretory Cells

Suberization has been suggested as a general mechanism for providing diffusion barriers as a result of natural physiological and developmental process (Kolattukudy 1980). Investigations of glands in higher plants have revealed specialized cell wall incrustations that are situated strategically for separating cells from plant apoplast. The material in most cases has been considered to be suberin or cutin and its possible importance is in restricting backflow of secreted material (Schnepf 1974).

Rachmilevitz and Fahn (1973) studied the ultrastructure of nector-secreting cells in two species of *Vinca* and one of *Citrus* and described an 'inner cuticle' lining the large intercellular spaces between parenchyma cells that were close to the epidermis.

Upon maturation, single cell trichomes on the petioles, stipules, and young leaves of creosote bush (*Larrea tridentata* Car.) senesce, collapse and extrude degraded cell material (Thomson et al. 1979). Prior to maturation these trichomes become isolated symplastically and apoplastically from other leaf cells by the deposition of a suberin layer internal to the trichome primary wall (Thomson et al. 1979).

Marion and Fahn (1979) described a lamellated suberin layer in the wall of mature oil cells in *Laurus nobilus* leaves. After the deposition of the suberin wall layer, plasmodesmata became occluded with a homogenous electron-opaque material and a state of complete separation of the mature oil cell from the surrounding cells developed.

TEM micrographs produced by Olesen (1979) revealed the ultrastructure of the cuticular envelope in salt glands of *Frankenia pauciflora*. In specialized three-dimensional ring structures that form around transfusion areas of gland cells thin suberin-like or cutin-like lamella released by the plasmalemma were seen to coalesce into the amorphous mass of the cuticular envelope. They postulated that wax or wax precursors (polar fatty acids) used the plasmalemma as a template to form the various structural incrustations. After separation from the plasalemma, the thin lamella would then become coated with macromolecular polyesters of hydroxy-fatty acids, fatty acids and phenolic acids - the chief components of cutin and suberin.

Wattendorf (1976) reported that leaves of *Agave americana* L. contained suberized idioblasts with one to few styloids (i.e., calcium oxalate crystals). The primary wall of the styloid containing idioblasts was suberized and lamellate on the innermost part. Where crystals did not touch the wall a suberin sheath continuous with the wall suberin layer was deposited around the crystal.

Seed Coats

Seed development involves the inward flow of chemicals via vascular channels attached to a concurrently developing seed coat. Upon seed maturation, the seed coat becomes a diffusion barrier and connections with vascular tissue are severed. Apparently, suberin in many cases is the phytopolymer that develops in the hilum region of the maturing seed.

Using cytological evidence Spurny (1964) described the deposition of suberin adcrustations on the apical part of cell walls of macrosclereids in the seed coat of the pea (*Pisum sativum* L.). The chalazal region, an area of the seed coat which may be regarded as an area of water influx,

did not show substantive suberin adcrustations for the case of mature seeds, and water penetration was almost twice as fast as that of the smooth part of the seed coat where suberin adcrustations were abundant in the macrosclereids.

Zee and O'Brien (1970) suggested the identity of an electron-translucent layer of adcrusting substance in the cell walls of the pigment strand of wheat caryopsis at 9 days after anthesis to be suberin.

Espelie et al. (1980) examined the thick-walled cells in the chalazal region of the inner seed coat for grapefruit (*Citrus paradisi* Macfed.) and described a lamellar structure similar to that of suberized walls lining "hollow heart" regions in potato tubers (Dean et al. 1977). By using gas-liquid chromatography and mass spectrometry the identity of components for the chalazal lamellar deposits were revealed and were reported to strongly support previous guidelines set for distinguishing the chemical nature of suberin (Kolattukudy 1980). Espelie et al. (1980) reported that seed root resistance to water vapor diffusion was greater for suberized regions (Rt. = 192 s/cm) than for the cutin-bearing non-chalazal region (Rt. = 62 s/cm) in grapefruit seeds.

Bundle Sheath Cells

Internal leaf blade anatomy has been used to develop taxonomic schemes for grass tribes. Brown (1958) microscopically examined the internal anatomy of leaf blades of 101 species in 72 genera and used the absence or presence of endodermis and the characteristics of the parenchyma bundle sheath and of the surrounding mesophyll cells as criteria to help differentiate six groups of grasses. Some grasses were reported as having both an inner mestome sheath (or endodermis) and an outer parenchyma bundle sheath surrounding each vascular bundle with other

grasses only having a parenchyma bundle sheath.

Excluding members of the Bambuseae and a comparatively small number of grasses having mixed characteristics, Metcalfe (1960) was able to divide grasses into a festucoid or panicoid group depending upon leaf structure. Although there were some intermediates, panicoid grasses were generally characterized by having one sheath surrounding vascular bundles whereas festucoid grasses had two.

Carolin et al. (1973) conducted a study using light microscopy and TEM on mature leaves of Gramineae species and used the presence or absence of an osmiophilic layer in the walls of parenchyma bundle sheaths and mestome sheaths as criteria to help characterize six types of internal grass leaf anatomy. Panicoid and Eragrostoid anatomy types were described as those grass leaves having an osmiophilic layer in the parenchyma bundle sheath. These osmiophilic layers were found to extend only around the outer tangential and parts of the radial walls for cells in the parenchyma bundle sheaths. Panicoid types of leaf anatomy described by Carolin et al. (1973) have been shown to occur in those grasses with a C_4 photosynthetic pathway (Hatch and Slack 1970; Downton and Tregunna 1968; Laetsch 1971). Osmiophilic layers in the parenchyma bundle sheath walls were suggested to have an important function in maintaining a compartmentalization of the pentose-phosphate pathway in the parenchyma bundle sheath and the C_4 pathway in the mesophyll, but evidence has been provided raising questions on the effectiveness of this function (Carolin et al. 1973; Laetsch 1974). Laetsch (1974) points out that adaptive aspects of sheath or Kranz anatomy have generally been concerned with carbon flow and this may have led researchers astray as to the more significant causal relationships (e.g., functional adaptations to xeric or

saline environments). O'Brien and Carr (1970) observed an electron-transparent layer in the cell walls and completely encircling each cell of the mestome sheath for wheat and oat leaves. A similar structure was reported in the walls of the parenchyma bundle sheath of maize leaves. Both structures were reported to contain 3 to 4 thin lamella appearing in plasmodesmata regions. They assumed the lamella to be suberin and noted that they appeared to constrict each plasmodesmata such that the membrane that lines the plasmodesmatal canal would be pressed against the electron-dense lumen that ocupies the canal. O'Brien and Carr (1970) suggested that the suberin lamella modifies the role of the canal in these plasmodesmata. In parts of the junction between tracheary elements and parenchyma bundle sheaths in maize a suberin layer was sometimes absent even when such a layer was readily distinguishable in the radial and other tangential walls of the same cell (O'Brien and Carr 1970).

Apparently, the development of suberin layers in cell wall regions of parenchyma bundle sheaths and mestome sheaths that abut vascular elements of leaves is prevented depending upon the immediate type of vascular cell, development stage of the bundle, and species concerned, thus reflecting the maintenance of a particular physiological state (O'Brien and Carr 1970; Kuo et al. 1974; O'Brien and Kuo 1975; Evert et al. 1978; Eleftheriou and Tsekos 1979). Kuo et al. (1974) reported that the regulation of water movement between vascular tissue and mesophyll of wheat leaves was an unlikely function of the suberin lamella in the mestome sheath cells. Instead, suberinized walls were assigned a role of being passive barriers to the diffusion of sugar through the free space, forcing a symplastic flux of sugars into the stele and securing a separation between this inward directed flow of sugars and an outward directed flow of water from

the xylem.

Methods of Chemical Identification

Reliable chemical methods for suberin component quantitation and elucidations on the exact chemical nature of suberin are only now being realized. As suberin is tightly associated with other polymeric materials in the cell wall, isolation in a pure form is difficult. As is usually the case, treatment of tissue samples with hydrolytic enzymes and organic solvents produces 'enriched' preparations of suberin (Kolattukudy and Agrawal 1974; Kolattukudy and Dean 1974; Robards et al. 1976).

Few methods are available for the depolymerization of suberin. Among these are 1) alkaline hydrolysis 2) transesterification with sodium methoxide or boron trifluoride in absolute methanol 3) hydrogenolysis with $LiAlH_4$ in tetrahydrofuran (Kolattukudy 1980). Hydrogenolysis with $LiAlD_4$ has proved to be useful because of the introduction of deuterium to specifically-labeled functional groups such as ketones, aldehydes, and epoxides present in the polymer (Kolattukudy 1980). Thin layer chromatography (TLC) traditionally has been used to separate the mixture of monomers obtained from depolymerization into different chemical classes (e.g., hydrocarbons, wax esters, fatty alcohols, etc.). Similarly, combined gas-liquid chromatography and mass spectrometry (GLC-MS) has been widely used following TLC in order to separate the homologous series in each fraction obtained from TLC. Mass spectra provide adequate information about the identity of monomers due to specific cleavages in aliphatic carbon chains at such functional groups as methyl groups, carbonyl groups, and hydroxyl groups (Kolattukudy 1980). Once "suberin-enriched" preparations have been treated with the

depolymerization techniques, much of the insoluable material left is colored residue. Colored, water-soluable phenolic compounds are also discharged. These phenolic components of suberin cannot be readily isolated due to the similar bonding patterns to those found in lignin. As a result, methods such as alkaline nitrobenzene or CuO oxidation and treatment with aqueous or acidic dioxane under high temperature and pressure must be used so that the molecular-bonding pattern will be cleaved and soluable phenolic products from suberin obtained (Kolattukudy 1981).

Aliphatic Components

Recent studies indicate aliphatic components constitute 5 to 30% of the "suberin-enriched" preparations (Kolattukudy et al. 1975, Kolattukudy 1981). The major aliphatic monomers are ω-hydroxy acids, the corresponding dicarboxylic acids, very long chain fatty acids, and C_{20} to C_{30} fatty alcohols.

Kolattukudy et al. (1975) were able to depolymerize and fractionate into phenolic and aliphatic components the suberized tissue in roots of carrots (*Daucus carota*), parsnip (*Pastinaca sativa*), rutabaga (*Brassica napobrassica*), turnip (*Brassica rapa*), red beet (*Beta vulgaris*), and sweet potato (*Ipomoea batatas*). Thin layer chromatography of the aliphatic fractions resulted in the following major separations: fatty alcohols (3-6%), ω-hydroxy acids (29-43%), dicarboxylic acids (16-27%), and fatty acids (4-18%). Combined GLC-MS was used to identify components of these major groups of monomers. Of the ω-hydroxy acid components, 18-hydroxy-octadec-9-enoic acid predominated in all plants, except rutabaga, where quantities of this ω-hydroxyacid were equal to quantities of 16-hydroxy-hexadecanoic acid (42% each). Dicarboxylic acids predominantly consisted

of C_{16} and C_{18} diacids with octa-9-ene-1,18-dioic acid for all plants except rutabaga being the major diacid (45-81%). The rutabaga fraction contained hexadecane-1,16-dioic acid as the major dicarboxylic acid. Very long chain fatty acids (> C_{20}) predominated in all six plants and of the fatty alcohols, C_{18}, C_{20}, C_{22}, and C_{24} saturated primary alcohols predominated in all six plants.

By using similar methods, wound-healing tissue in potato tubers (*Solanum tuberosum*), Jade leaves (*Crassula argentea*), tomato fruit (*Lycopersicon esculentum* var. Bonny Best) and bean pods (*Phaseolus vulgaris* var. Bonus) were analyzed for the aliphatic components of suberin (Kolattukudy and Dean 1974; Dean and Kolattukudy 1976). Fatty acids (C_{16} - C_{22}), fatty alcohols (C_{16} - C_{26}), octadec-9-ene-1,18-dioic acid and 18-hydroxy-octa-9-enoic acid were identified to be major components of the aliphatic fraction in wound periderm of potato tubers (Kolattukudy and Dean 1974). The hydrogenolysis of the wound periderm of tomato fruit produced hexadecane-1,16-diol and octadec-9-ene-1,18-diol which were derived from a 1:1 mixture of the ω-hydroxy acids and dicarboxylic acids of the corresponding chain lengths (Dean and Kolattukudy 1976). The major aliphatic component in the hydrogenolysate for wound material in bean pods was octadecene-1,18-diol, but smaller amounts of hexadecane-1,16-diol and long-chain alcohols were also isolated (Dean and Kolattukudy 1976). Jade leaves on hydrogenolysis gave octadecene-1,18-diol, C_{16} and C_{22} diols, as well as alcohols from C_{16} to C_{26} (Dean and Kolattukudy, 1976). Dean and Kolattukudy (1976) suggested that even though cutin is the natural protective barrier of aerial plant parts, the healing of injuries to most plants may involve only suberin deposition. Authors further commented that their results on the identification of aliphatic monomers for wound-healing tissue supported a

previously proposed basis for classifying phytopolymers as cutin and suberin (Kolattukudy et al. 1975) major distinctions were indicated as the predominance of polar, in-chain hydroxylated and/or epoxy acids for major aliphatic components of cutin, whereas ω-hydroxy acids and dicarboxylic acids were major for suberin. Tentative guidelines for distinguishing cutin and suberin reported in more recent papers have deviated little from that (Espelie and Kolattukudy 1979; Kolattukudy 1981). Presented in Table A-1 are distinguishing monomers reported by Kolattukudy (1981).

Table A-1. Differences in composition for cutin and suberin.

Monomer	Cutin	Suberin
Dicarboxylic acids $HOOC(CH_2)_n\ COOH$	minor	major n=14-20
In-chain-substituted acids	major	minor*
$CH_2\ (CH_2)_x\underset{OH}{CH}(CH_2)_y\ COOH$	y=8,7,6, or 5 x+y=13	
$CH_2\ (CH_2)_7\underset{OH}{CH}\text{-}\underset{O}{CH}(CH_2)_7COOH$		
$CH_2\ (CH_2)_7\underset{OH}{CH}\text{-}\underset{OH}{CH}(CH_2)_7COOH$		
Very long chain acids $CH_3\ (CH_2)_n\ COOH$	rare and minor	common and substantial n=20-26
Very long chain alcohols $CH_3\ (CH_2)_nCH_2OH$	rare and minor	Common and substantial n=18-30
Phenolics	Low	High

* In some cases substantial

Epidermal and endodermal tissues from the first internode of etiolated sorghum (*Sorghum bicolor*) seedlings can be separated from each other and individually subjected to suberin depolymerization techniques (Espelie and Kolattukudy 1979). Using combined gas-liquid chromatography and mass spectrometry, characteristic aliphatic monomers indicating cutin and suberin were present in those isolated fractions from epidermis and endodermis, respectively (Espelie and Kolattukudy 1979). Similarly, Espelie et al. (1980) isolated the aliphatic components of the cutin and suberin phytopolymers from the inner seed coat of grapefruit and reported a confirmation of the typical constituents for each. In another study, Espelie and Kolattukudy (1979) compared the aliphatic components for the lipid layer in the bundle sheath cell walls of *Zea mays* leaves with those in the cuticular layer of the same plant. All constituents supported the criteria for cutin and suberin except for mid-chain hydroxy and epoxy acids which were present in the suberin fraction in substantial amounts, thus indicating a possible variability in this major structural feature. Results of the analysis of the major alkanes extracted with chloroform from the bundle sheath cells indicated that wax may be associated with suberin in providing a role for a diffusion barrier. Wax has been indicated to represent the light band component of the alternating dark band-light band complex typical of the cell wall suberin layer (Soliday et al. 1979). Treatment of the lamellate structure in potato tuber periderm with trichloroacetate (TCA), an inhibitor of wax synthesis, results in a disruption of the suberin lamella (Soliday et al. 1979). Progressive increases in TCA concentrations applied to developing potato tuber periderm caused a corresponding decrease in the number of light bands and a disruption of the regular spacing between

bands (Soliday et al. 1979). Treatment of periderm with TCA severely inhibited the development of hydrocarbons and fatty alcohols, but had no effect on the accumulation of the major aliphatic components of suberin. Resistance to the diffusion of water vapor was decreased as concentration of TCA increased, thereby indicating the crucial role that waxes have as a diffusion barrier in association with the suberin phytopolymer. Dark bands of the ultrastructure of suberin have been postulated to represent a phenolic matrix linked by ω-hydroxyoctadecenoic acid and the corresponding dicarboxylic acids while light bands have been postulated to represent wax accumulation as a result of hydrophobic channels formed from the crosslinking of the phenolic matrix and aliphatic components with long chain fatty acids and alcohols (Soliday et al. 1979).

Phenolic Composition

Information on the phenolic composition of suberin is scant. Riley and Kolattukudy (1975) isolated phenolic fractions from "suberin-enriched" preparations from periderm in potato, sweet potato, turnip, rutabaga, carrot, and red beet. Experimental techniques used resulted in a small quantity (≅ 1% of the mass) identified as esterified ferulic acid which was suggested to be originally covalently bonded to suberin. Techniques applicable for lignin chemistry have been applied to "suberin-enriched" preparations and major phenolic fractions have been recovered, but they have not yet been fully characterized (Kolattukudy 1981).

Suberin Structure

Approximate suberin compositions of potato periderm have been reported to be: carbohydrates, 50%; phenolics, 40-45%; aliphatics 5-10% (Kolattukudy 1981). Based on limited studies on suberin composition, Kolattukudy (1981) has proposed a working hypothesis on the structure of suberin (Fig. A-1).

According to the model, the phenolic matrix, similar in structure to lignin, is attached to cell wall carbohydrates on one side and cross-linked with aliphatic components on the other.

The ω-hydroxy acids and dicarboxylic acids, which make up the majority of the aliphatics, provide the hydrophobic conditions necessary for the interaction of waxes. Thus, a possible explanation for the typical dark-light lamellar ultrastructure of suberin can be realized (Soliday et al. 1979).

Figure A-1. A tentative model proposed by Kolattukudy (1981) for suberin structure.

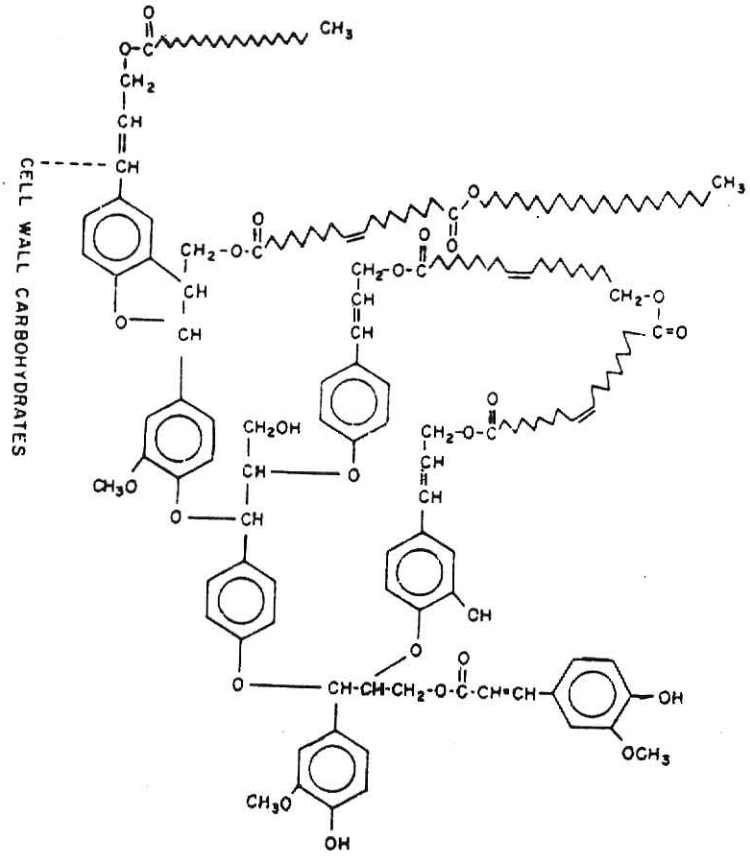

A REVIEW OF THE LITERATURE II. RUMEN MICROBIAL DEGRADATION PATTERNS OF SUBERIN-AFFILIATED TISSUES IN GRASS LEAF BLADES

Information on the manner in which rumen microorganisms attack and degrade plant cell walls with direct reference to suberin is non-existent in the literature. Studies on rumen microbial patterns of degradation in relation to differently-arranged and structured grass leaf tissues are only now being reported (Akin 1979). The following is a review on the rumen microbial degradation patterns on suberin-affiliated tissues in leaf blades of grasses.

Early light-microscopy work has shown that some forage tissues are not digested in the rumen by bacteria (Drapala et al. 1947; Baker and Hariss 1947). Light microscopic work showed attachment of rumen bacteria to cell walls of forage tissue as well as clear zones of degraded tissue surrounding unattached bacteria (Baker and Hariss 1947). Using transmission electron microscopy (SEM) and scanning electron microscopy (SEM) Akin et al. (1974) were able to observe microbial attachment and non-attachment to cell walls in leaf tissues of the C_4 plant 'Coastal' bermudagrass [*Cynodon dactylon* (L.) Pers] incubated *in vitro* with rumen fluid for 6, 12, and 72 hr. Attachment of bacteria did not seem to be necessary at times for the degradation of the thin cell walls of phloem and mesophyll. In that case, the activity of extracellular enzymes, for at least partial degradation of these tissues, was considered to be adequate. Attachment appeared necessary, however, for the degradation of bundle sheaths and epidermis. Attachment was accompanied by an extracellular matrix surrounding large cocci bacteria, but was apparently direct for bacillus and small cocci.

Akin and Amos (1975) observed microbial degradation on leaf tissues

collected from Kentucky-31 tall fescue plants after 4 weeks of summer regrowth. Again, attachment to the cell walls of more resistant tissue (e.g., bundle sheaths, epidermis, and sclerenchyma) was observed for several morphological types of bacteria. Authors postulated that the necessity of attachment to bundle sheaths and epidermis for digestion and the apparent neglect of attachment to phloem and mesophyll for digestion indicates why those forages with a greater proportion of mesophyll and phloem are more digestible.

Akin (1980), using TEM, was able to quantitate the morphological types of bacteria attached to cell walls in leaf tissues of 'Coastal' bermudagrass, Kentucky-31 tall fescue (*Festuca arundinacea* Schreb.), and 'Boone' orchardgrass (*Dactylis glomerata* L.) incubated *in vitro* with rumen fluid for 6, 12, 24 and 72 hr. An irregular-shaped bacilli and an encapsulated cocci made up ≅ 70% of the morphological types observed to be attached to cell walls. The ratio of encapsulated cocci to irregular-shaped bacilli did not change with the ease of digestibility for different plant tissue types, but apparently the manner of digestion did. For example, attachment prior to digestion was not observed for parenchyma bundle sheaths in orchardgrass, but it apparently served as a prerequisite for parenchyma bundle sheath breakdown in 'Coastal' bermudagrass.

Vascular bundles of coastal bermudagrass are characterized as having an inner mestome sheath and an outer parenchyma bundle sheath with walls usually thicker than the mesophyll (Metcalfe 1960; Carolin et al. 1973). Both sheaths lack any prominent osmiophilic layer in their cell walls (Carolin et al. 1973). Orchardgrass and *Festuca* species, however, have been reported to have walls of the parenchyma bundle sheath as thin as the mesophyll walls and an osmiophilic layer completely encircling the

the cells of the mestome sheath (Carolin et al. 1973).

Akin and Burdick (1975) estimated the percent of tissue types for leaf blades of various tropical and temperate grasses and related it to the ease of *in vitro* degradation. Although the leaf anatomy varied for the forages observed, patterns of microbial degradation on leaf blade sections from plants of 4-week summer regrowth were generally similar for both warm-season and cool-season species. The ease of digestion generally followed the sequence of phloem and mesophyll > epidermis and parenchyma bundle sheaths > sclerenchyma and lignified vascular tissue (i.e., xylem and inner bundle sheath when present). That pattern with slight variations has been followed as indicated by SEM observations on rumen incubations of leaf material from *Andropogon* species (Brazle et al. 1979), smooth bromegrass (*Bromus inermis*) and tall fescue (Harbers et al. 1981), and ensiled corn and sorghum (Harbers and Thouvelle 1980). After 72 hr of *in vivo* incubation, leaf sections from bluestem plants (109 days postemergence) showed poorly digested epidermis and spongy mesophyll, xylem, and cuticle sloughings (Brazle et al. 1979). Mesophyll was degraded early for both smooth bromegrass and tall fescue leaves (75 to 80 days postemergence), but phloem remained intact longer for fesuce (Harbers et al. 1981). Even though tissues were considered to be removed at a faster rate for rumen microbial degradation of ensiled corn and sorghum leaves compared to unfermented plant leaves, epidermis was poorly digested at 72 hr (Harbers and Thouvenelle 1980). *Zea* and *Sorghum* species have a panicoid type of internal leaf anatomy characterized by lacking a mestome sheath, but having a well developed parenchyma bundle sheath (Metcalfe 1960) often containing an osmiophilic layer presumed to be suberin (O'Brien and Carr 1970; Espelie and Kolattukudy 1979; Evert et al. 1978) in the outer tangential and radial walls (Carolin et al. 1973).

Latham et al. (1978a) examined the initial patterns of adhesion of the cellulolytic bacterium, *Ruminococcus flavefaciens*, in pure culture on leaf sections of perennial ryegrass (*Lolium perenne* L.) which had on osmiophilic layer completely encircling the cells in the mestome sheath of leaves (Carolin et al. 1973). In early stages of digestion (1.5 hr) with pures cultures of *R. flavefaciens* major sites of adhesion were restricted to cut or damaged surfaces of plant cell walls. Observations of tissue digested for 3, 6, and 9 hr revealed epidermis and phloem to be tissues digested earliest followed by mesophyll and sclerenchyma. After 9 hr of incubation, no adhesion occurred for chloroplastic membranes, plant cuticle, and cell walls for metaxylem, protoxylem, and inner (mestome) sheaths. Latham (1978b) also demonstrated different propensities for various leaf tissues of perennial ryegrass by mixed cultures of *Bacteroides succinogenes* and *R. flavefaciens*.

Even though ratios of the amounts of epidermis and parenchyma bundle sheaths to the amounts of mesophyll and phloem were higher for tropical grasses than for temperate grasses, amounts of lignified, nondigestible tissues were similar for leaf blades of both grass types (Akin and Burdick 1975). Akin and Burdick (1975) suggested that the reason tissues in warm-season grasses were more slowly digested than those of cool-season grasses was due to differences in amounts of tissue types along with differences in the inherent structural rigidity of these tissues. Parenchymal bundle sheaths (outer sheaths), in particular, were reported to be more resistant to microbial degradation in warm-season grasses than were the outer sheaths of temperate grasses. At 12 hr of incubation none of the parenchyma bundle sheath cells for dallisgrass (*Paspalum dilatatum* Poir.) were degraded, whereas 97-100% was degraded for orchardgrass, smooth bromegrass, and

Kentucky bluegrass (*Poa pratensis* L.). The internal leaf anatomy of dallisgrass is panicoid type and consists of an osmiophilic layer (probably suberin) embedded in the radial and outer tangential walls of a well-developed parenchyma bundle sheath; mestome sheaths are absent (Metcalfe 1960; Carolin et al. 1973). Orchardgrass and Kentucky bluegrass, however, have Pooid type of internal leaf anatomy characterized by having parenchyma bundle sheaths with cell walls no thicker than mesophyll walls and mestome sheaths with cell walls completely lined by an osmiophilic layer (Carolin et al. 1973).

Akin and Burdick (1977) used TEM and SEM to examine ultrastructural factors affecting the microbial removal of starch in parenchyma bundle sheath cells of leaf blade sections collected from 'Coastal' bermudagrass, 'Pensacola' bahiagrass (*Paspalum notatum* Flugge) and 'Pangola' digitgrass (*Digitaria decumbens* Stent) plants in a 4-week regrowth stage. After 6 hr of incubation in rumen fluid, mesophyll cells in all grasses were partially or completely degraded; parenchyma bundle sheath cells were intact. Most starch grains, if not all, were present in chloroplasts of the parenchyma bundle sheath and hydrolysis of this starch did not occur until the rigid sheath cell wall had been degraded by rumen microbes. Micrographs often showed hydrolysis of starch grains without bacteria seen close by. Authors suggested that the slowly degraded cell walls of the parenchyma bundle sheath in C_4 plants acts as a barrier towards bacterial utilization of starch and other intracellular nutrients and may be a contributing factor in causing lower nutritive values for some warm-season grasses as compared to cool-season grasses. *Paspalum* and *Digitaria* species have panicoid type of internal leaf anatomy (Carolin et al. 1973).

Barton and Akin (1977) used SEM to reveal the effect of delignification by chemical treatment on the *in vitro* degradation (1, 2, 4, 6, 24, and

48 hr) of leaf blade tissues with rumen fluid for Kentucky-31 tall fescue harvested at 4-weeks summer regrowth. For delignified sections, inner bundle sheaths were reported to be separated from nonlignified tissues; some collapsed cells in the mesophyll were noted. The extent of digestion of delignified leaf sections, when subjected to microbial degradation, was greater for all tissues except vascular bundles when compared with untreated grass samples. They reported that because large delignified vascular bundles were not degraded the indigestibility of this tissue must be partly due to a property of the cell wall polysaccharides.

Akin and Burdick (1979) conducted histochemical tests on leaf tissues of 'Coastal' bermudagrass and Kentucky-31 tall fescue and provided evidence that those tissues (e.g., xylem and inner bundle sheath) that stain positive with acid phloroglucinol are more resistant to microbial degradation. Sclerenchyma which was degraded at the periphery was chlorine-sulfite positive. Parenchyma bundle sheaths of bermudagrass and parenchyma bundle sheaths and mesophyll of tall fescue stained positive for chlorine-sulfite, but the reaction faded within a few minutes. Authors concluded that forage tissues contain different types of lignin with each type modifying the rate of cell wall breakdown in a different degree.

Other research has related results from histochemical tests on different lignin types in leaf tissues of several grass species to the relative ease of digestibility (Akin and Burdick 1981). In general, mestome sheaths and xylem of grasses subjected to *in vitro* fermentation with rumen fluid [i.e., bermudagrass, Kentucky-31 tall fescue, orchardgrass, 'Clair' timothy (*Phleum pratense* L.)] resisted break down and stained positive for acid phloroglucinol lignin. Mestome sheaths of certain grasses, however, reacted with both acid phloroglucinol and

chlorine-sulfite which indicated that both coniferaldehyde and syringyl residues were present in these cell walls.

Summary

Tissue quality and quantity and specific microanatomy of forages are important factors to consider when determining patterns of rumen microbial degradation. Suberin deposits along vascular tissues of many forages should certainly be embodied within those confines.

LITERATURE CITED

Akin, D.E. 1980. Evaluation by electron microscopy and anaerobic culture of types of rumen bacteria associated with digestion of forage cells walls. Appl. Environ. Microbiol. 39:242-252.

Akin, D.E. 1979. Microscopic evaluation of forage digestion by rumen microorganisms - a review. J. Animal Sci. 48:701-710.

Akin, D.E. and H.E. Amos. 1975. Rumen bacterial degradation of forage cell walls investigated by electron microscopy. Appl. Microbiol. 29:692-701.

Akin, D.E. and D. Burdick. 1981. Relationships of different histochemical types of lignified cell walls to forage digestibility. Crop Sci. 21:577-581.

Akin, D.E. and D. Burdick. 1979. Histochemical and electron microscopic observations of lignified cell walls in forage grasses as related to digestibility. J. Animal Sci. 49:39.

Akin, D.E. and D. Burdick. 1977. Rumen microbial degradation of starch-containing bundle sheath cells in warm-season grasses. Crop Sci. 17:529-533.

Akin, D.E. and D. Burdick. 1975. Percentage of tissue types in tropical and temperate grass leaf blades and degradation of tissues by rumen microorganisms. Crop Sci. 15:661-668.

Akin, D.E., D. Burdick, and G.E. Michaels. 1974. Rumen bacterial interrelationships with plant tissue during degradation revealed by transmission electron microscopy. Appl. Microbiol. 27:1149-1156.

Baker, F. and S.T. Hariss. 1947. The role of the microflora of the alimentary tract of herbivora with special reference to ruminants. No. 2. Microbial digestion in the rumen (and caecum) with special reference to the decomposition of structural cellulose. Nutr. Abstr. Rev. 16:3-12.

Barton, II, F.E. and D.E. Akin. 1977. Digestibility of delignified forage cell walls. J. Agric. Food Chem. 25:1299-1303.

Bonnett, H.T. 1968. The root endodermis: fine structure and function. J. Cell Bio. 37:199-205.

Brazle, F.K., L.H. Harbers, and C.E. Owensby. 1979. Structural inhibitors of big and little bluestem digestion observed by scanning electron microscopy. J. Animal Sci. 48:1457-1463.

Brown, W. 1958. Leaf anatomy in grass systematics. Bot. Gaz. 119: 170-8.

Clarkson, D.T. and A.W. Robards. 1975. "The endodermis; its structural development and physiological role." In: The Development and Function of Roots. ed. by J.G. Torrey and D.T. Clarkson, Academic Press. London.

Carolin, R.C., S.W.L. Jacobs, and M. Vesk. 1973. The structure of cells of the mesophyll and parenchymatous bundle sheath of the Gramineae. Bot. J. Linn. Soc. 66:259-275.

Dean, B.B. and P.E. Kolattukudy. 1976. Synthesis of suberin during wound-healing in jade leaves, tomato fruit, and bean pods. Plant Physiol. 58:411-416.

Dean, B.B., P.E. Kolattukudy, and R.W. Davis. 1977. Chemical composition and ultrastructure of suberin from hollow heart tissue of potato tubers (*Solanum tuberosum*). Plant Physiol. 59:1008-1010.

Downton, W.J.S. and E.B. Tregunna. 1978. Carbon dioxide compensation - its relation to photosynthetic reactions, systematics of the Gramineae, and leaf anatomy. Can. J. Bot. 46:200-215.

Drapala, W.J., L.C. Raymond, and E.W. Crampton. 1947. Pasture studies XXVII: The effects of maturity of the plant and its lignification and subsequent digestibility by animals as indicated by methods of plant history. Sci. Agr. 27:36-41.

Eleftheriou, E.P. and I. Tsekos. 1979. Development of mestome sheath cells in leaves of *Aegilops comosa* var. *thessalica*. Protoplasma. 100:139-153.

Esau, K. 1965. Plant Anatomy. Wiley, New York.

Espelie, K.E. and P.E. Kolattukudy. 1979. Composition of the aliphatic components of suberin of the endodermal fraction from the first internode of etiolated sorghum seedlings. Plant Physiol. 63: 433-35.

Espelie, K.E., R.W. Davis, and P.E. Kolattukudy. 1980. Composition, ultrastructure, and function of the cutin- and suberin- containing layers in the leaf, fruit peel, juicesac, and inner seed coat of grapefruit (*Citrus paradisi* Macfed). Planta. 149:498-511.

Evert, R.F., W. Eschrich, and W. Heyser. 1978. Leaf structure in relation to solute transport and phloem loading in *Zea mays* L. Planta 138:279-294.

Ferguson, I.B. and D.T. Clarkson. 1976. Ion uptake in relation to the development of a root hypodermis. New Phytol. 77:11-14.

Ferguson, I.B. and D.T. Clarkson. 1975. Ion transport and endodermal suberization in the roots of *Zea mays*. New Phytol. 75:69.

Hatch, M.D. and C.R. Slack. 1970. "The C_4 dicarboxylic acid pathway of photosynthesis." In: Progress in Phytochemistry. 2:35-106. ed. by L. Reinhold and Y. Liwschitz. Academic Press, London.

Harbers, L.H. and M.L. Thouvenelle. 1980. Digestion of corn and sorghum silage observed by scanning electron microscopy. J. Animal Sci. 50:514-526.

Harbers, L.H., F.K. Brazle, D.J. Raiten, and C.E. Owensby. 1981. Microbial degradation of smooth brome and tall fescue observed by scanning electron microscopy. J. Animal Sci. 51:439-446.

Kolattukudy, P.E. 1981. Structure, biosynthesis, and biodegradation of cutin and suberin. Ann. Rev. Plant Physiol. 32:539-567.

Kolattukudy, P.E. 1980. "Cutin, suberin, and waxes." In: The Biochemistry of Plants. 4:571-645. ed. by P.K. Stumpf and E.E. Conn. Academic, New York.

Kolattukudy, P.E. and V.P. Agrawal. 1974. Structure and aliphatic constituents of potato tuber skin (suberin). Lipids 9:682-691.

Kolattukudy, P.E. and B.B. Dean. 1974. Structure, gas chromatographic measurement, and function of suberin synthesized by potato tuber tissue slices. Plant Physiol. 54:116-121.

Kolattukudy, P.E., K. Kronman, A.J. Polouse. 1975. Determination of structure and composition of suberin from the roots of carrot, parsnip, rutabaga, turnip, red beet, and sweet potato by combined gas-liquid chromatography and mass spectrometry. Plant Physiol. 55:567-573.

Kuo, J., T.P. O'Brien, and M.J. Canny. 1974. Pit-field distributions, plasmodesmatal frequency and assimilate flux in the mestome sheath cells of wheat leaves. Planta 121:97-118.

Laetsch, W.M. 1974. The C_4 syndrome: a structural analysis. Ann. Rev. Plant Physiol. 25:27-52.

Laetsch, W.M. 1971. "Chloroplast structural relationships of C_4 plants." In: Photosynthesis and Photorespiration. ed. by M.D. Hatch, C.B. Osmond, and R.O. Slayter. Wiley-Interscience, New York. p. 323-349.

Latham, M.J., B.E. Brooker, G.L. Pettipher, and P.J. Harris. 1978a. *Ruminococcus flavefaciens* cell coat and adhesion to cotton cellulose and to cell walls in leaves of perennial ryegrass (*Lolium perenne*). Appl. Environ. Microbiol. 35:156-165.

Latham, M.J., B.E. Brooker, G.L. Pettipher, and P.J. Harris. 1978b. Adhesion of *Bacteroides succinogenes* in pure culture and in the presence of *Ruminococcus flavefaciens* to cell walls in leaves of perennial ryegrass (*Lolium perenne*). Appl. Environ. Microbiol. 35:1166-1173.

Marion, R. and A. Fahn. 1979. Ultrastructure and development of oil cells in *Laurus nobilus* leaves. Bot. J. Linn. Soc. 78:31-40.

Metcalfe, C.R. 1960. Anatomy of the Monocotyledons. I. Gramineae. Oxford Univ. Press, London.

O'Brien, T.P. and D.J. Carr. 1970. A suberized layer in the cell walls of the bundle sheath of grasses. Aust. J. Biol. Sci. 23:275-287.

O'Brien, T.P. and J. Kuo. 1975. Development of the suberized lamella in the mestome sheath of wheat leaves. Aust. J. Bot. 23:783-794.

Olesen, P. 1979. Ultrastructural observations on the cuticular envelope in salt glands of *Frankenia pauciflora*. Protoplasma 99:1-9.

Olesen, P. 1978. Studies on the physiological sheaths in roots. I. Ultrastructure of the exodermis in *Hoya carnosa* L. Protoplasma 94:325-340.

Peterson, C.A., R.A. Peterson, and A.W. Robards. 1978. A correlated histochemical and ultrastructural study of the epidermis and hypodermis of onion roots. Protoplasma 94:325-340.

Rachmilevitz, T. and A. Fahn. 1973. Ultrastructure of nectaries of *Vinca rosea* L., *Vinca major* L. and *Citrus sinensis* Osbeck cv. Valencia and its relation to the mechanism of nectar secretion. Ann. Bot. 37:1-9.

Riley, R.G. and P.E. Kolattukudy. 1975. Evidence for covalently attached p-coumaric acid and ferulic acid in cutins and suberins. Plant Physiol. 56:650-654.

Robards, A.W., H.L. Payne, and B.E.S. Gunning. 1976. Isolation of the endodermis using wall-degrading enzymes. Cytobiologie 13:85-92.

Robards, A.W., S.M. Jackson, D.T. Clarkson, and J. Sanderson. 1973. The structure of barley roots in relation to the transport of ions into the stele. Protoplasma 77:291-311.

Schnepf, E. 1974. "Gland cells." In: Dynamic Aspects of Plant Ultrastructure. ed. by A.W. Robards. McGraw-Hill Book Co., London.

Schonherr, J. and H. Ziegler. 1980. Water premeability of *Betula* periderm. Planta 147:345-354.

Soliday, C.L., P.E. Kolattukudy, and R.W. Davis. 1979. Chemical and ultrastructural evidence that waxes association with the suberin polymer constitute the major diffusion barrier to water vapor in potato tuber (*Solanum tuberosum* L.). Planta 146:607-614.

Spurny, M. 1964. Changes in the permeability of the seed coat in connection with the development of suberin adcrustations of the macrosclereids from the seed coat of the pea (*Pisum sativum* L.). Flora 154:547-567.

Tippet, J.T. and T.P. O'Brien. 1976. The structure of eucalypt roots. Aust. J. Bot. 24:619-632.

Thomson, W.W., K.A. Platt-Aloia, and D. Koller. 1979. Ultrastructure and development of the trichomes of *Larrea* (creosote bush). Bot. Gaz. 140:1249-1260.

Wattendorf, J. 1976. Ultrastructure of the suberized styloid cells in *Agave* leaves. Planta 128:163-165.

Wilson, A.J. and A.W. Robards. 1978. The ultrastructural development of mechanically impeded barley roots. Effects on the endodermis and pericycle. Protoplasma 95:255-265.

Zee, S.Y. and T.P. O'Brien. 1970. Studies on the ontogeny of the pigment strand in the caryopsis of wheat. Aust. J. Biol. Sci. 23:1153-1171.

Appendix Part III

The following figures are a composite of light and transmission electron micrographs obtained from the present study.

Abbreviations Used in Figures

abe = abaxial epidermis

ade = adaxial epidermis

b = bulliform cells

bs = bundle sheath

bsc = bundle sheath cell

bscw = bundle sheath cell wall

c = chloroplast

m = mesophyll

mc = mesophyll chloroplast

mcw = mesophyll cell wall

mx = metaxylem

p = phloem

pi = pit field

pr = protozoa

pxl = protoxylem lacunea

s = sclerenchyma

sg = starch grains

sl = suberin lamella

x = xylem

xcw = xylem cell wall

Figure A-1. Light micrograph of an undigested leaf blade of big bluestem (20 days postemergence). Bar = 50 μm.

Figure A-2. Light micrograph of a cross section of a leaf blade of big bluestem (20 days postemergence) removed from the rumen after 16 hr of incubation showing the start of mesophyll disruption. Bar = 20 μm.

Figure A-3. Light micrograph of a vascular bundle and parenchyma bundle sheath of indiangrass (20 days postemergence) removed after 16 hr of rumen incubation. Few mesophyll chloroplasts and cell walls remain intact. Xylem and phloem tissue are still visible. Bar = 10 μm.

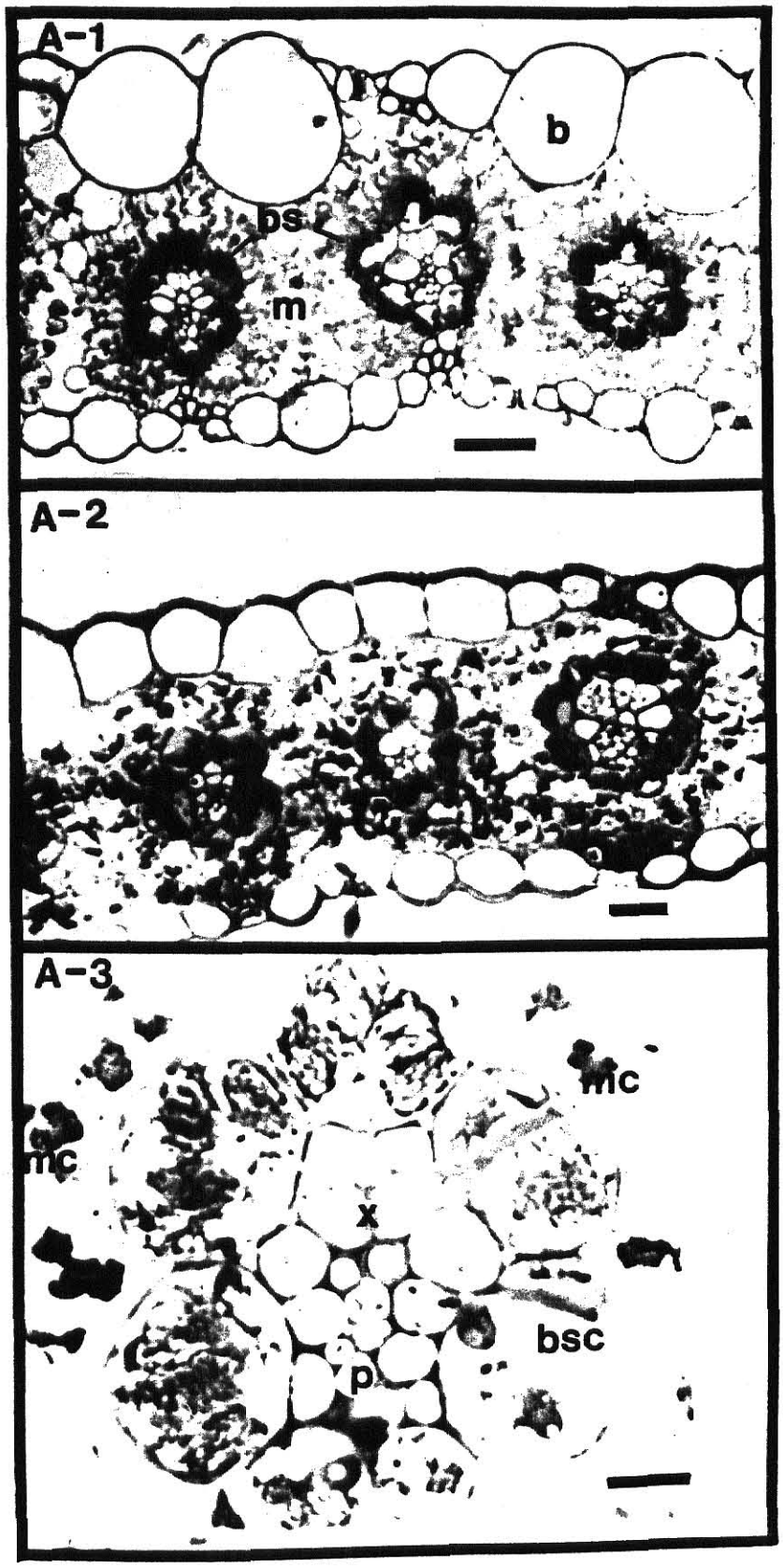
A-1
b
bs
m
A-2
A-3
mc
mc
x
bsc
p

Figure A-4. Light micrograph of a big bluestem leaf sample (20 days postemergence) removed from the rumen after 32 hr showing signs of degradation to all leaf tissues. Bar = 10 μm.

Figure A-5. Light micrograph of an indiangrass leaf sample (20 days postmergence) removed from the rumen after 32 hr of incubation. Mesophyll, phloem, and inner cell walls of both epidermis layers are degraded. Outer cell walls of parenchyma bundle sheath cells appear to have "sprung" open perhaps caused by areas in the cell wall least resistant to microbial degradation (i.e. plasmodesmata) coupled with stress from rumen contractions. Bar = 50 μm.

Figure A-6. Light micrograph of a large lateral vascular bundle of indiangrass (20 days postemergence) removed from the rumen after 64 hr of incubation. Xylem and sclerefied tissue is all that remains. Bar = 20 μm.

Figure A-7. Light micrograph of an undigested leaf blade cross section from indiangrass (140 days postemergence). Chloroplasts are still abundant in the parenchyma bundle sheaths and mesophyll. Bar = 50 μm.

Figure A-8. Light micrograph of a vascular bundle and surrounding tissue of an indiangrass leaf sample (140 days postemergence) after 8 hr of rumen incubation. Mesophyll cell walls are starting to show signs of degradation. Bar = 20 μm.

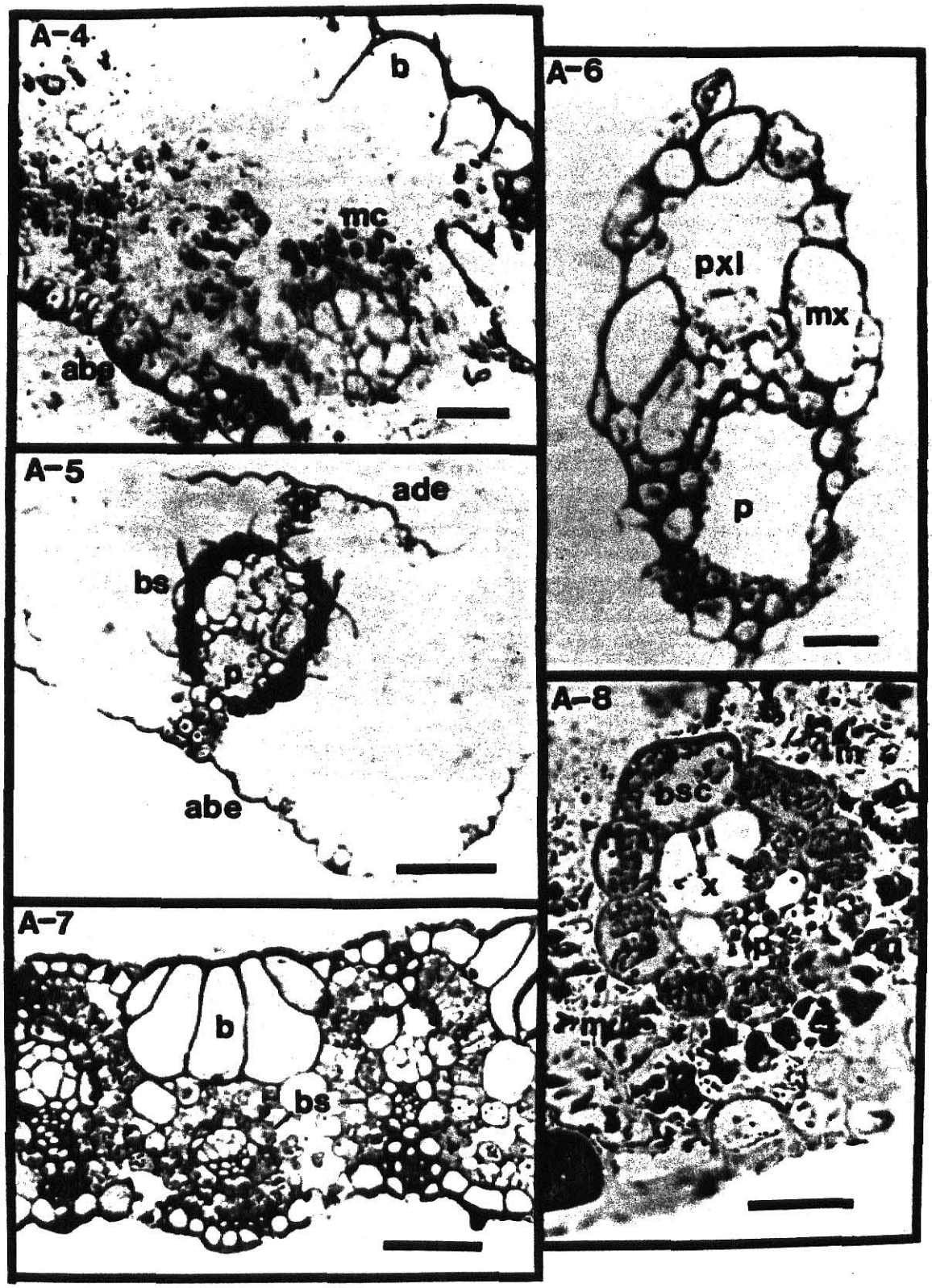
A-4
b
mc
abe
A-5
ade
bs
p
abe
A-6
pxl
mx
p
A-8
m
bsc
x
p
m
A-7
b
bs

Figure A-9. Light micrograph of a vascular bundle and surrounding tissue from an indiangrass leaf sample (140 days postemergence) after 16 hr of rumen incubation. Cellular contents of the parenchyma bundle sheaths are starting to clear as surrounding mesophyll shows signs of less degradation. Bar = 20 μm.

Figure A-10. Light micrograph showing extensive degradation to leaf tissues from an indiangrass sample (140 days postemergence) subjected to 64 hr of rumen incubation. Abundant fragments of mesophyll tissue remain. Bar = 100 μm.

Figure A-11. Light micrograph of a leaf blade cross section from indiangrass (140 days postemergence) after 64 hr of rumen microbial degradation. Portions of most tissues except phloem remain. Note the large unobstructed spaces formed by the protoxylem lacunea, metaxylem vessels, and digested phloem which may provide avenues for relatively rapid rumen microbial distribution. Bar = 50 μm.

Figure A-12. Light micrograph of a large lateral vascular bundle and surrounding tissue from a big bluestem leaf blade (140 days postemergence) after 64 hr of rumen incubation. Note that phloem, one of the tissues reported generally to be digested early, is still present. Bar = 50 μm.

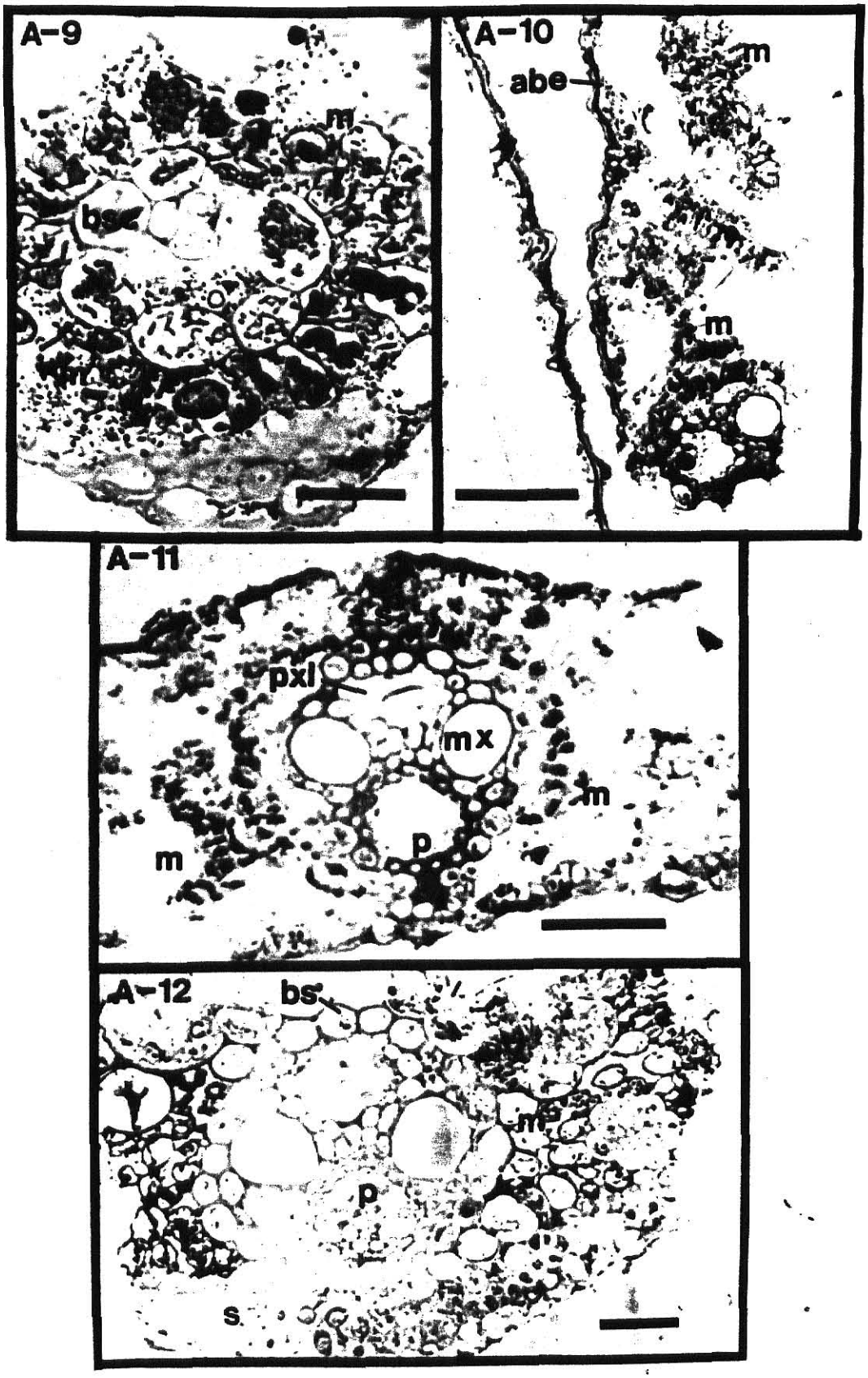
A-9
m
bs
A-10
abe
m
m
A-11
pxl
mx
m
m
p
A-12
bs
m
p
s

Figure A-13. Light micrograph of a leaf cross section from indiangrass (140 days postemergence) subjected to 64 hr of rumen incubation. Large proportions of all leaf tissues are present. Several protozoa are shown. Bar = 100 μm.

Figure A-14. Light micrograph of a leaf cross section from indiangrass (140 days postemergence) subjected to 96 hr of rumen incubation. Dark stained chloroplasts can still be seen within many of the mesophyll cells. Bar = 100 μm.

Figure A-15. Light micrograph of sclerenchyma and vascular tissue from a big bluestem leaf sample (140 days postemergence) remaining after 128 hr of rumen degradation. Some parenchyma bundle sheath cells still remain. Phloem has been degraded. Bar = 20 μm.

Figure A-16. Light micrograph showing xylem, sclerenchyma, and phloem remaining for an indiangrass leaf sample after 128 hr of *in vivo* rumen degradation. Parenchyma bundle sheath cells are missing. Bar = 50 μm.

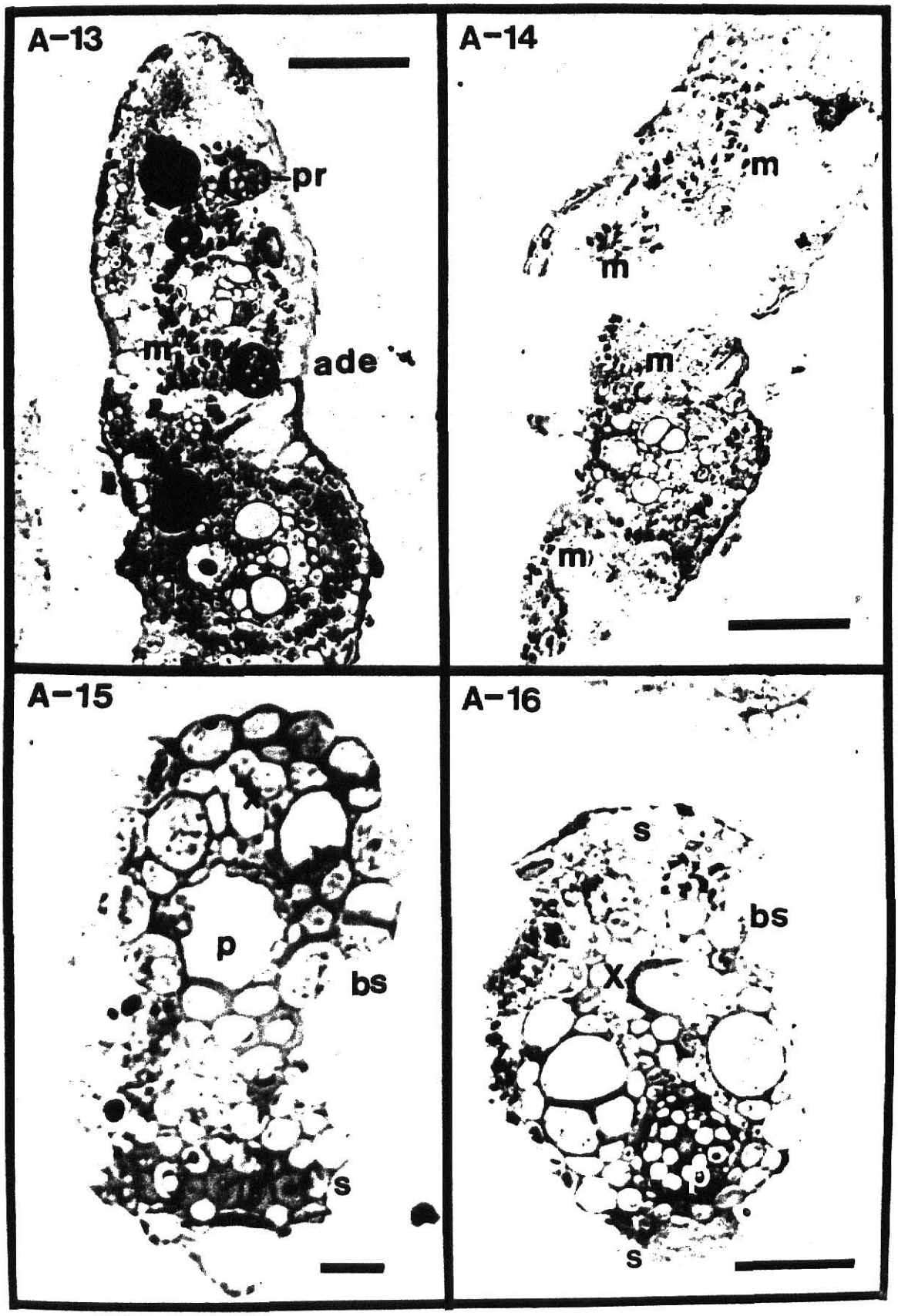
A-13
pr
m
m
ade
A-14
m
m
m
m
A-15
p
bs
s
A-16
s
bs
x
p
s

Figure A-17. Transmission electron micrograph (TEM) showing numerous starch grains within parenchyma bundle sheath cells of a big bluestem leaf sample (20 days postemergence) after 2 hr of *in vivo* degradation. Bacteria are absent from view, but some digestion is occurring as evident by hydrolysis of the peripheral portions of chloroplasts and the cell walls of mesophyll. Bar = 2 μm.

Figure A-18. Outer tangential cell wall of a parenchyma bundle sheath cell from a big bluestem leaf sample (20 days postemergence) subjected to 8 hr rumen degradation (TEM). Numerous cocci and bacillus bacteria are prevalent on the mesophyll side of the suberin lamella whereas none can be seen inside the parenchyma bundle sheath cell where starch grains are still visible. Bar = 1 μm.

Figure A-19. Outer tangential cell wall of a parenchyma bundle sheath cell from a big bluestem leaf section (20 days postemergence) subjected to 16 hr of rumen incubation (TEM). An electron-translucent suberin layer can be seen (arrow) running through several pit fields located between thin mesophyll cell walls and the thicker parenchyma bundle sheath cell wall. A solitary coccoid bacterium can be seen within the parenchyma bundle sheath cell. Bar = 0.5 μm.

Figure A-20. Rumen microorganism present in a phloem cell that abuts the inner tangential wall of a parenchyma bundle sheath cell (TEM). Some hydrolysis appears to have occurred to the region of cell wall common to both phloem and parenchyma bundle sheath cell in conjunction with the nearby bacterium. No suberin lamella can be seen. The section is of a big bluestem leaf blade sample (20 days postemergence) after 16 hr of rumen incubation. Bar = 1 μm.

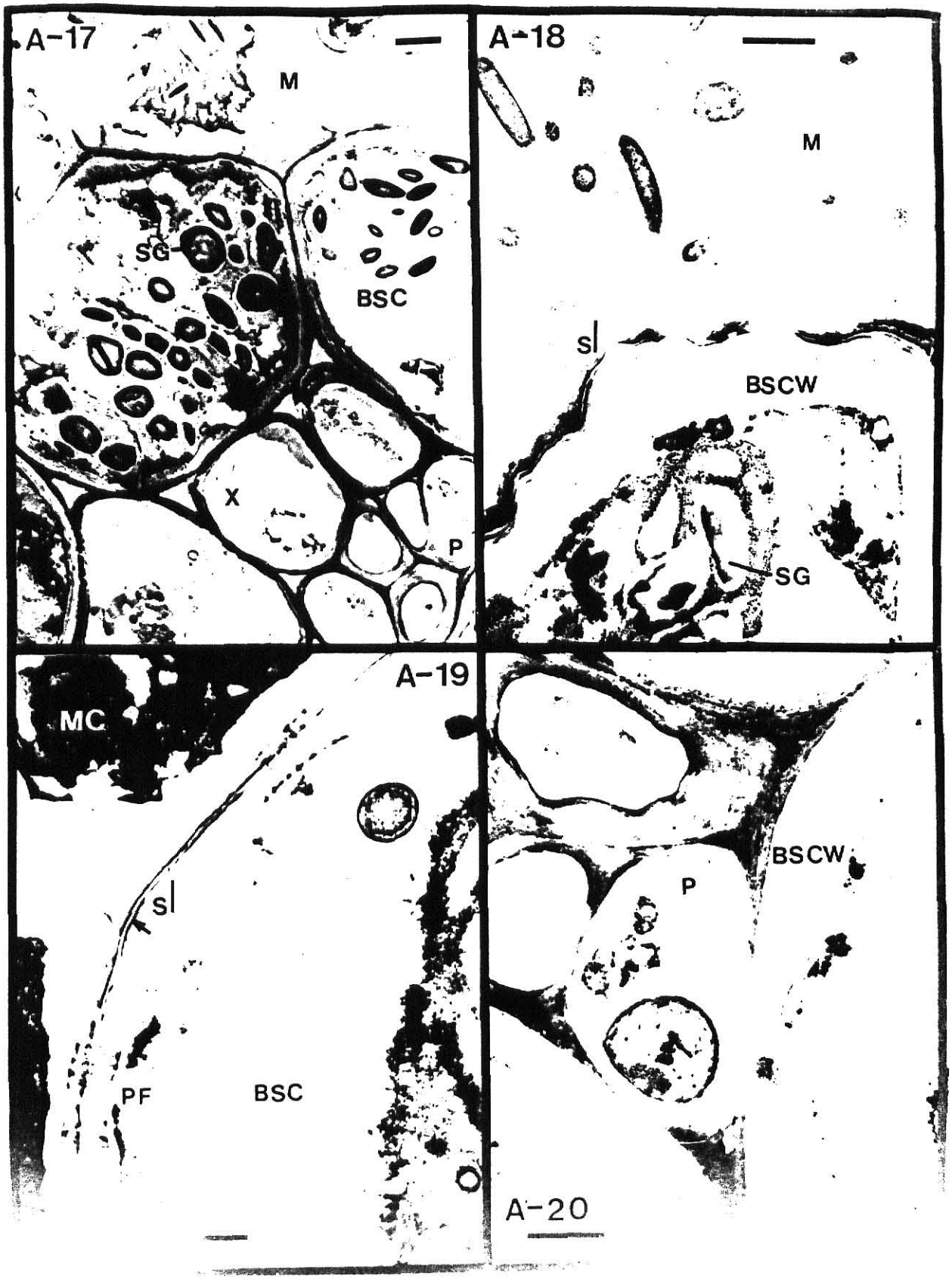
A-17
M
SG
BSC
X
P
A-18
M
SI
BSCW
SG
A-19
MC
SI
PF
BSC
BSCW
P
A-20

Figure A-21a. Portions of the inner and outer tangential cell walls and radial cell wall of a parenchyma bundle sheath taken from a leaf section of indiangrass (140 days postemergence) subjected to 1 hr of rumen digestion. Rectangular areas labeled X and Y are magnified in figures A-21b and A-21c, respectively. Bar = 1 μm.

Figure A-21b. A higher magnification of area X outlined in figure A-21a. No suberin lamella can be seen between the xylem cell wall and parenchyma bundle sheath cell wall. Bar = 0.5 μm.

Figure A-21c. A higher magnification of area Y outlined in figure A-21a. An electron-translucent suberin lamella can be readily distinguished between the cell walls of the parenchyma bundle sheath and mesophyll. Bar = 0.5 μm.

Figure A-22. Strand of suberin with attached cell wall components remaining after a big bluestem leaf sample (140 days postemergence) was subjected to 16 hr of rumen incubation. Parenchyma bundle sheath cell wall material is scarce whereas mesophyll cell wall and cytoplasmic material are more abundant. Bar = 0.5 μm.

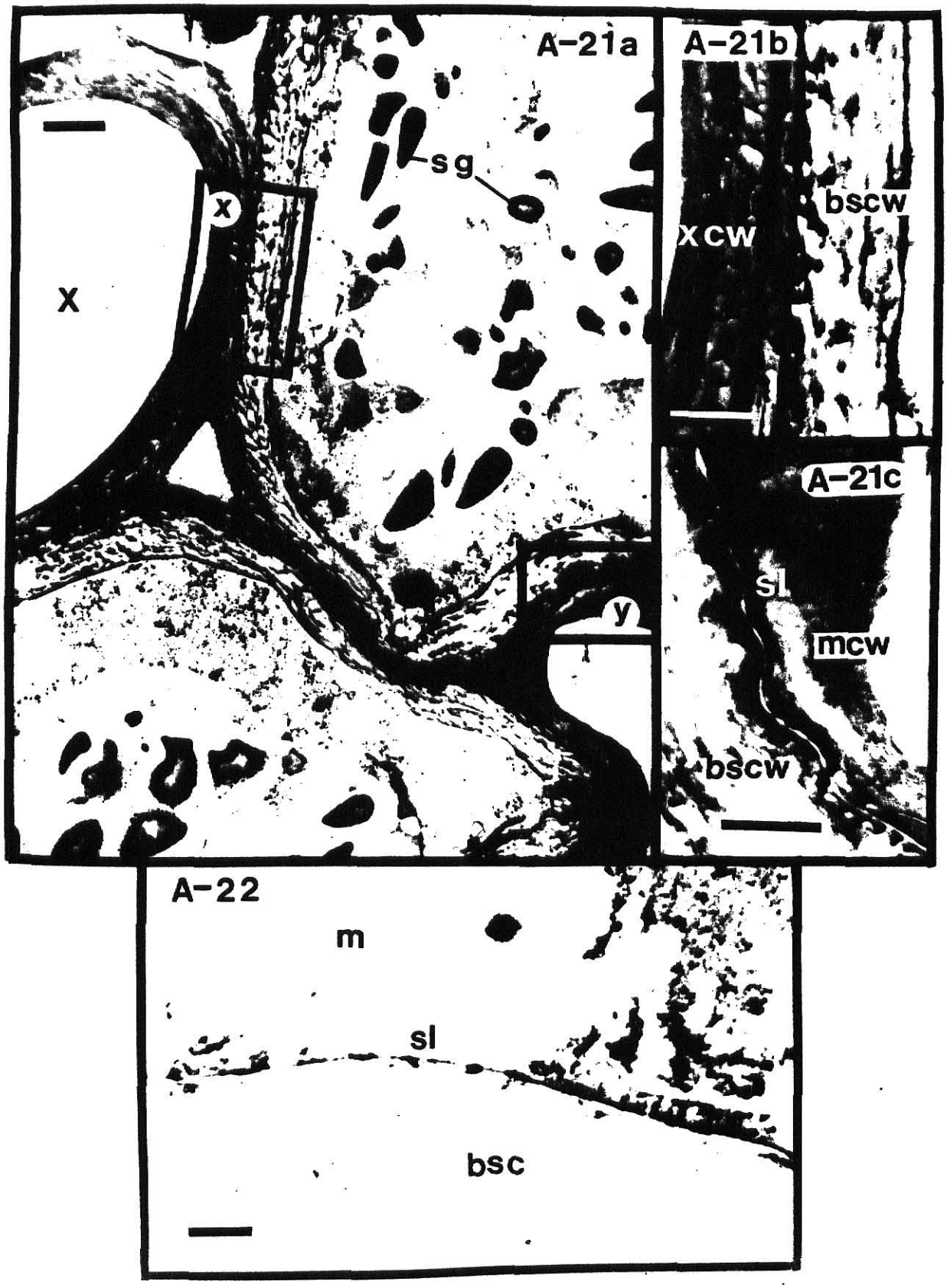
A-21a
x
x
sg
y
A-21b
xcw
bscw
A-21c
sl
mcw
bscw
A-22
m
sl
bsc

Figures A-23a and A-23b. Upper and lower halves, respectively, of a big bluestem vascular bundle (140 days postemergence) after 16 hr of *in vivo* degradation. Abundant rumen microorganisms can be seen in xylem, phloem, and parenchyma bundle sheath cells. Starch grains within the parenchyma bundle sheath cells are still present, but show some signs of hydrolysis. Bars = 2 μm.

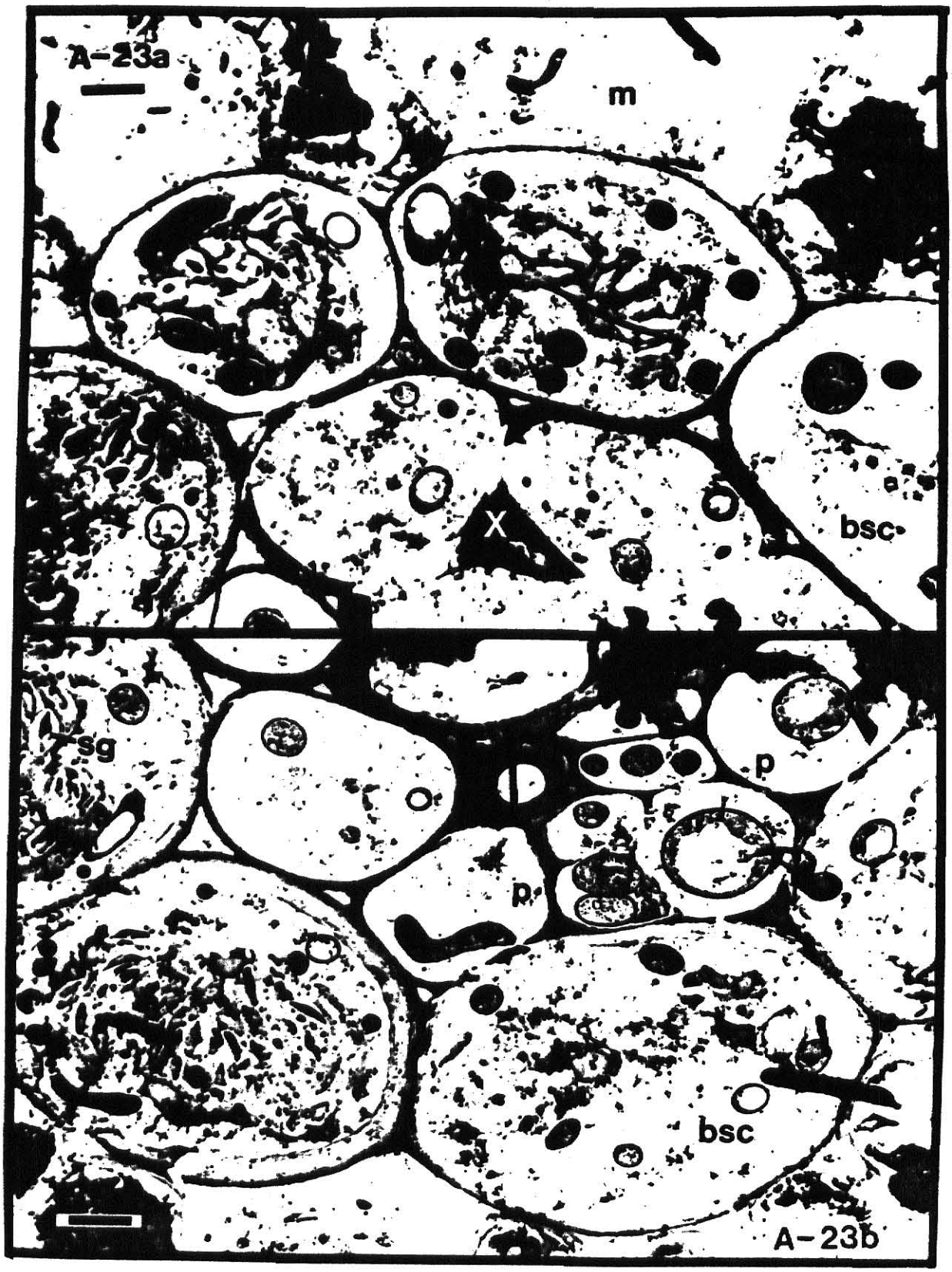
A-23a
m
X
bsc
sg
p
p
bsc
A-23b

Figure A-24. Hydrolysis of a radial cell wall of a parenchyma bundle sheath cell from a big bluestem leaf section (140 days postemergence) after 32 hr of rumen incubation. Note the separation of cell wall material from the suberin lamella which remains intact extending beyond, into, and through the pit field region. Bar = 0.5 μm.

Figure A-25. Bacteria aggregated in the pit field cavity located between two parenchyma bundle sheath cell walls of a big bluestem leaf sample (140 days postemergence) after 32 hr of rumen incubation. The suberin layers are visible separating the two parenchyma bundle sheath cell walls, but they cannot be detected in the plasmodesmata. Bar = 0.2 μm.

Figure A-26. Plasmodesmata connecting a mesophyll cell with a bundle sheath cell from an indiangrass leaf sample (140 days postemergence) after 16 hr of rumen incubation. Cell wall material from mesophyll remains, but bundle sheath cell wall has been hydrolyzed. Electron-opaque occlusions in the desmotubule of the plasmodesmata extend out into the hydrolyzed region of the bundle sheath cell wall perhaps indicating a relatively greater resistance to rumen microbial degradation. Bar = 0.2 μm.

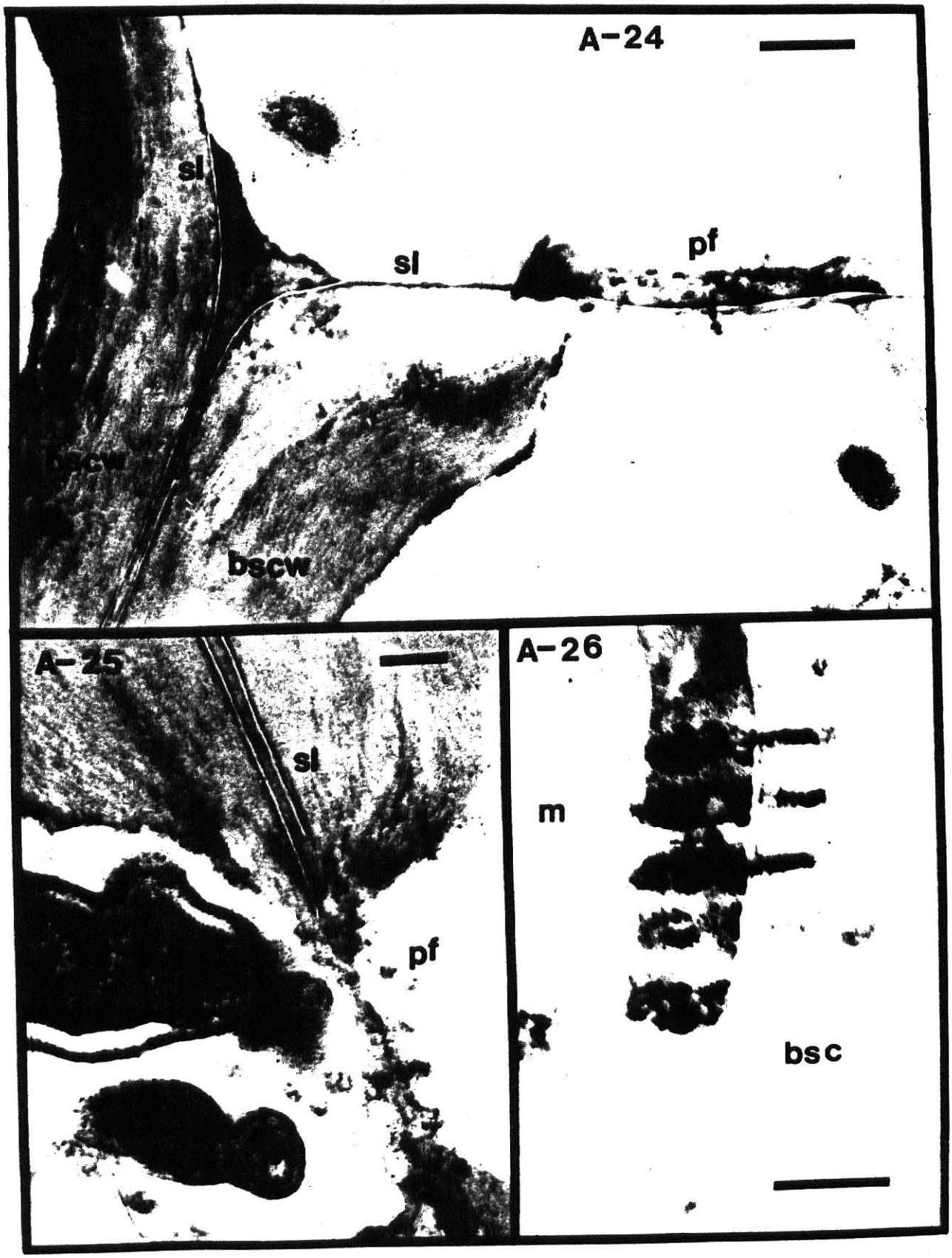
A-24
sl
sl
pf
bscw
A-25
sl
pf
A-26
m
bsc

Figure A-27. TEM of vascular tissues and bundle sheath cells of an indiangrass leaf section (140 days postemergence) after 128 hr of rumen incubation. Extent of rumen degradation to chloroplasts and starch grains within bundle sheath cells deviates little from those of bundle sheath cells subjected to shorter rumen incubation times (see figures A-23a and A-23b). Bar = 2 μm.

Figure A-28. Vascular tissue and bundle sheath cells of a big bluestem leaf sample (140 days postemergence) after 128 hr of rumen incubation. Bacteria are numerous within vascular cells, but starch grains within the bundle sheath cells show signs of only slight degradation. Bar = 3 μm.

Figure A-29. Suberin lamella of an outer tangential cell wall of a parenchyma bundle sheath cell from an indiangrass leaf sample (140 days postemergence) after 128 hr of *in vivo* degradation. Cell wall material has been removed from outside the suberin lamella by bacteria, but parenchyma bundle sheath wall shows signs of little damage. Bar = 0.2 μm.

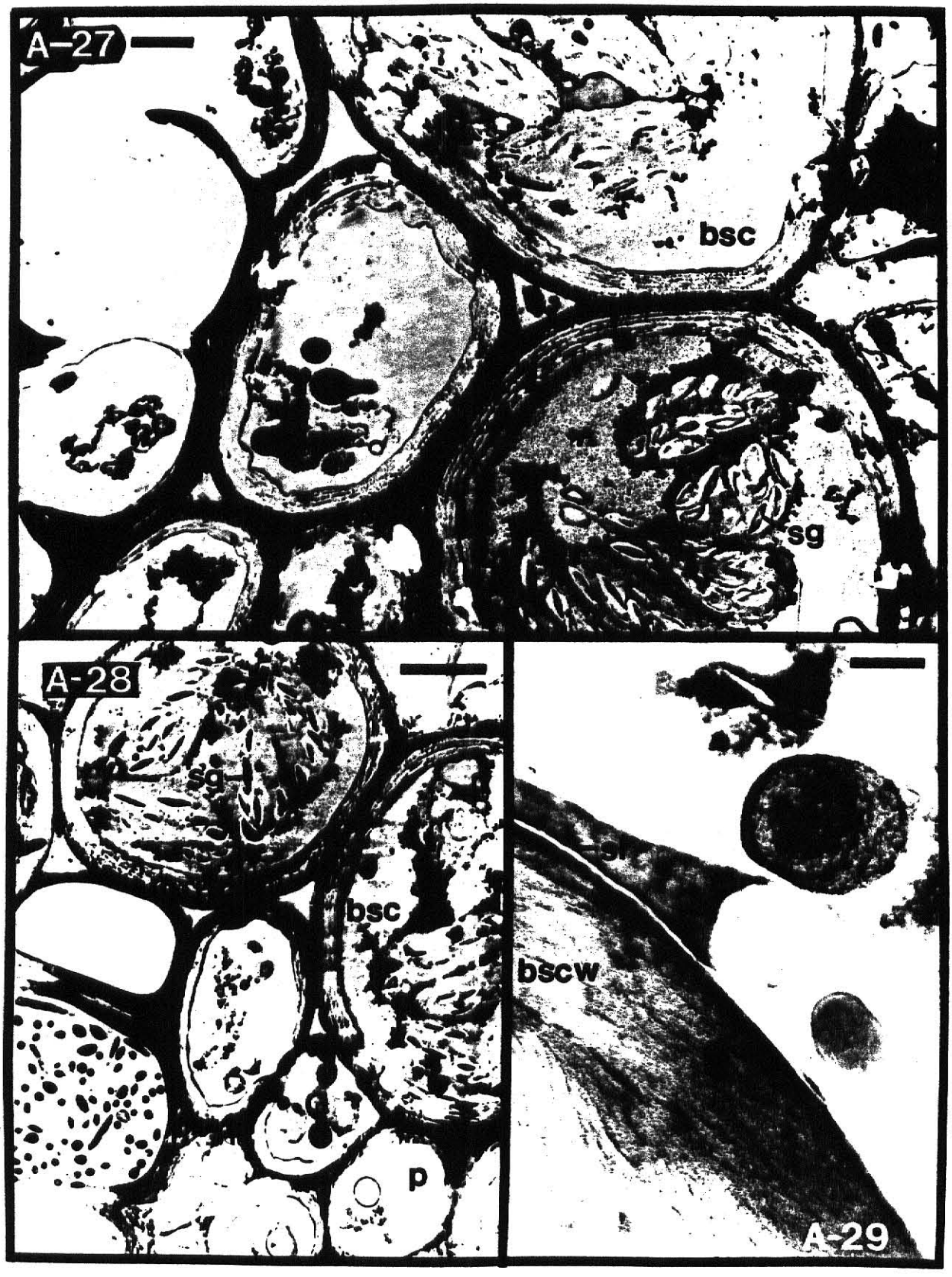
A-27
bsc
sg
A-28
sg
bsc
p
bscw
A-29

BUNDLE SHEATH SUBERIN LAYER AS A BARRIER TO RUMEN MICROBIAL DEGRADATION IN INDIANGRASS AND BIG BLUESTEM LEAF BLADES

by

ARTHUR A. HASTERT

B. S., Kansas State University, 1978

AN ABSTRACT OF A MASTER'S THESIS

submitted in partial fulfillment of the

requirements for the degree

MASTER OF SCIENCE

Department of Agronomy

KANSAS STATE UNIVERSITY
Manhattan, Kansas

1982

ABSTRACT

Light and transmission electron microscopy was used to observe amounts of tissues in undigested leaf samples and rates of tissue disappearance in rumen digested leaf samples for big bluestem (*Andropogon gerardi* Vitman) and indiangrass [*Sorghastrum nutans* (L.) Nash] in two different growth stages. Undigested late-spring (20 days postemergence) leaf blades contained slightly higher parenchyma bundle sheath areas than did undigested late-summer (140 days postemergence) leaf blades. Mesophyll was seen to remain in digested leaf sections for at least until 16 and 32 hr of incubation (50 to 75% degraded) for plants in late-spring growth stages. In digested leaf samples from plants in late-summer growth stages mesophyll remained until 96 and 128 hr of incubation (50 to 75% degraded). Parenchyma bundle sheaths tended to resist degradation more so than did mesophyll and was most noticeable in late-summer leaf blades subjected to 128 hr of *in vivo* incubation where only 25 to 50% of bundle sheath cells were degraded. Numerous starch grains were observed in bundle sheath cells for leaf blades of both grasses in both growth stages, but hydrolysis of starch grains did not occur until bundle sheath walls were disrupted.

High magnifications of outer tangential and radial walls of bundle sheath cells in digested leaf blades revealed a thin suberin layer that resisted degradation. Cell wall material with an adjoined suberin layer from a bundle sheath cell appeared undegraded depending upon the direction from which bacteria attacked. Late-summer digestion trials indicated differential degradation of vascular bundles. Light microscopy revealed extensive loss of phloem, xylem and parenchymal bundle sheath tissues for

small, less developed vascular bundles whereas larger more developed vascular bundles resisted digestion for incubation periods of 32 and 64 hr.